



# An Energy Efficient Radio Base Station

Lakshmi Prasad, Olof Bjerling  
1a5768pr-s@student.lu.se, tfy13obj@student.lu.se

Faculty of Engineering  
Lund University

## Supervisors:

Jonas Bengtsson, Ericsson, jonas.x.bengtsson@ericsson.com  
Joakim Persson, Ericsson, joakim.z.persson@ericsson.com  
Ulf Morland, Ericsson, ulf.morland@ericsson.com  
Johan Wernehag, LTH, johan.wernehag@eit.lth.se

## Examiner:

Pietro Andreani, LTH, pietro.andreani@eit.lth.se

August 24, 2018

© 2018  
Printed in Sweden  
Tryckeriet i E-huset, Lund

---

# Abstract

---

The mobile telecommunication network is growing year after year and it will soon move into the high speed 5G and Internet of Things technology. These new technologies will improve the throughput and data connectivity and due to that the energy consumption in radio and digital units may increase in a Radio Base Station (RBS). There are more than 500 000 off-grid RBSs in the world which are powered by diesel generators. This results in air pollution, green house gas emission and high fuel and maintenance costs for the operators. The main objective of this thesis is to find ways to bring down the energy consumption in radio and digital units and check the viability of a solar powered site instead of a diesel-powered site. This has been done for an LTE network. The current power save features developed by Ericsson has been studied and two new power save features have been implemented. The first is an innovative algorithm that optimizes the cooling in the baseband to obtain a minimal power consumption, this method was proved to work even in scenarios with large variations in ambient temperature. An Eco-mode algorithm was tried on few radio units, where the biasing of the power amplifiers was reduced in low load scenarios. This reduced the power consumption of each radio unit with up to 3.4% in the test cases described in the thesis. Finally, the design and economic analysis of a solar powered radio base station was performed, in order to recommend an energy efficient, sustainable and cost-effective option to mobile operators that would relieve the stress of regular maintenance and increased expenses. It showed that a combination of solar panels and diesel generator is the most economical and environment friendly solution.



---

## Acknowledgements

---

We would like to express our sincere gratitude to all our supervisors Jonas Bengtsson, Joakim Persson, Ulf Morland (Ericsson) and Johan Wernehag (LTH) for their timely guidance and support throughout the thesis. We would also like to thank Flemming Knudsen, manager PIR1G for giving us the opportunity to work on this thesis in the most well equipped lab at Ericsson. We also thank Anders Edman and Greger Bytström from Ericsson, Kista for sharing valuable information and suggestions on the different radios used in the thesis. Finally we would like to express our immense gratitude towards our families who stood as a great support during the thesis.

Olof Bjering and Lakshmi Prasad



---

## Popular Science Summary

---

### Towards Energy Efficient Mobile Networks

With the emergence of new mobile technologies and growing network, the necessity for energy efficient mobile networks becomes more and more significant. Energy efficient radio and digital units powered by environment friendly solar energy will be a better alternative to the current diesel generator powered base stations. As part of the thesis we have learned and worked with the hardware and software parts of the radio and baseband units. In order to come up with novel and innovative ideas to improve energy efficiency of radio and baseband units, a study of already available power save methods was done. There are different kinds of power save methods, some are pure optimizations where the base station uses less power without affecting the performance while others will intentionally reduce the performance in scenarios when and where maximum performance is not required. In the thesis there is one power save method of each kind, one that optimizes the use of cooling equipment in the baseband and one that reduces the power consumption in the radio at low load.

The baseband is the part of the radio base station that handles the logic and processing of the data. It contains electronic and electrical components within it and will therefore require a cooling equipment to protect it from overheating. For the baseband that was used in the thesis the cooling is performed by a fan connected to one side of the unit. The fan reads out the values from certain temperature sensors and will increase the fan speed if there is a risk of overheating. But another issue with high temperature is that it will increase the power consumption of the baseband due to thermal leakage. In order to decrease the temperature and thus the power consumption, the fan speed can be increased. This will however result in a higher power consumption for the fan itself. It was seen that one can find a fan speed for each scenario where the total power consumption is at its lowest. An innovative algorithm was implemented that continuously adjusts the fan speed in order to minimize the total power consumption.

The radio unit uses a bandwidth which allows it to transmit data at different frequencies. There is a power amplifier that can amplify the signal at all the available frequencies. In a lot of cases this is unnecessary since the load is much lower than the maximum throughput of the base station. A power save feature named ECO-mode was implemented that will reduce the biasing of the power amplifier. This limits the available throughput and it was used to save power in scenarios where the maximum throughput is not needed. An algorithm was developed that can turn on or off this mode depending on the load.

Installation of an off grid base station powered with a diesel generator is not only a costly affair but also an environment concern in that area. This problem can be reduced by using renewable energy sources that are pollution free and has lower costs in the long run. The steps to design a solar powered base station has been explained and analyzed in the thesis. A cost analysis was done with the three different power options; a fully solar, fully diesel and a combination of both to find the best alternative among them. The combined option was found to be most cost-effective among them. The optimal portion of each power source would give the lowest cost and this is individual to each location and power requirement of the site.



---

# Table of Contents

---

<b>1</b>	<b>Introduction</b>	<b>1</b>
1.1	Objectives and structure of report . . . . .	1
1.2	Telecommunication . . . . .	1
1.3	Radio Base Station . . . . .	2
1.4	Long Term Evolution . . . . .	3
<b>2</b>	<b>Energy Consumption</b>	<b>9</b>
2.1	Energy Efficiency Methods . . . . .	9
2.2	New methods . . . . .	13
<b>3</b>	<b>Baseband cooling</b>	<b>15</b>
3.1	Background . . . . .	15
3.2	Fan Power Consumption . . . . .	16
3.3	Optimal fan speed . . . . .	17
3.4	Adaptive fan speed . . . . .	18
3.5	Test method . . . . .	19
3.6	Results and comments . . . . .	19
3.7	Discussion . . . . .	21
<b>4</b>	<b>ECO-mode</b>	<b>23</b>
4.1	Background . . . . .	23
4.2	ECO-mode . . . . .	23
4.3	Scheduling . . . . .	24
4.4	Comparison of RUs . . . . .	25
4.5	Measurements in idle . . . . .	26
4.6	Measurements with load . . . . .	30
4.7	Adaptive mode . . . . .	40
<b>5</b>	<b>Off grid solar design</b>	<b>51</b>
5.1	Background . . . . .	51
5.2	Introduction . . . . .	51
5.3	Solar PV system . . . . .	55
5.4	Off-grid PV system design . . . . .	57
5.5	Cost analysis . . . . .	69

<b>6 Discussion</b>	<b>79</b>
6.1 Conclusions . . . . .	79
6.2 Other ideas . . . . .	80
6.3 Further steps . . . . .	82
<b>References</b>	<b>83</b>

---

## List of Figures

---

1.1	Mobile subscription per technology. The graph does not include Internet of Things (IoT) connections or Fixed Wireless Access (FWA) subscriptions [2]. . . . .	2
1.2	Schematic overview of the frequency domain for 1.4 MHz bandwidth. There are 6 resource blocks that consists of 12 subcarriers each and a guard band at both edges. . . . .	3
1.3	The resource grid for a 1.4 MHz bandwidth spanning over 10 sub-frames. There are 6 resource blocks in the frequency domain that all consists of 12 subcarriers of 15 kHz each. In time domain there are 10 TTIs all consisting of 14 symbols. These builds up the physical resource blocks that consists of 12 subcarriers and 14 symbols. There are coloured symbols in all PRBs, these are reference signals that will be explained later on. The image is generated through [3] . . . . .	4
1.4	Modulation scheme for QPSK, 16-QAM and 64-QAM. The angle and absolute value of the points corresponds to phase and amplitude of the wave [4]. . . . .	5
1.5	A PRB with no scheduled data. Image taken from [8]. . . . .	7
2.1	The power consumption at various loads for a typical RU. The load and power consumption are measured in percentage of their maxima. Measurements performed in the lab at Ericsson Lund. . . . .	10
3.1	The power consumption of the fan at different fan speeds. . . . .	16
3.2	Total power consumption measured for various fan speeds at different ambient temperatures. The lines are fitted second order polynomials and their corresponding R <sup>2</sup> -values are shown in the upper right box. . . . .	17
3.3	The graph at the top compares the power consumption of the base-band when the current fan control and the adaptive fan control methods are used. The difference between these graphs are then seen at the bottom. . . . .	20

4.1	Overview of an example with 10 resource blocks in frequency domain. In normal operation all PAs are biased, showed as "On" in the image. With backoff to the right there is a limit on the number of biased PAs and some are unbiased, showed as "Off". In this example the throughput is limited to 70% of its original value. This backoff can be used as an ECO-mode. . . . .	24
4.2	Power consumption for a radio A in idle mode and 40 W output power. The two graphs are showing the behaviour with and without Micro Sleep TX activated. . . . .	27
4.3	Power consumption for a radio B in idle mode and configured with 2 branches that has 40 W output power each. The two graphs are showing the behaviour with and without Micro Sleep TX activated. . . . .	28
4.4	Power consumption for a radio C in idle mode and 40 W output power. The two graphs are showing the behaviour with and without Micro Sleep TX activated. . . . .	29
4.5	Measurements for a radio A with Micro Sleep TX deactivated. The backoff is increased from 0 to 2.5 dB in steps of 0.1 dB. The top graph shows the power consumption, the middle the number of available PRBs and the lowest shows the resulting throughput. . . . .	32
4.6	Power savings from the ECO-mode in a radio A. The graphs shows scenarios with and without Micro Sleep TX and LESS. . . . .	33
4.7	Measurements for a radio B with Micro Sleep TX deactivated. The backoff is increased from 0 to 4.5 dB in steps of 0.1 dB. The top graph shows the power consumption, the middle the number of available PRBs and the lowest shows the resulting throughput. . . . .	34
4.8	Measurements of the throughput per power for the radio B and for various analog backoffs. The graph shows the ratio between the top and the bottom graph of figure 4.7. The high ratio at -2 dB means that the power is used efficiently. . . . .	35
4.9	Power savings from the ECO-mode in a radio B. The graphs shows scenarios with and without Micro Sleep TX and LESS. . . . .	36
4.10	Measurements for a radio C with Micro Sleep TX deactivated. The backoff is increased from 0 to 2.5 dB in steps of 0.1 dB. The top graph shows the power consumption, the middle the number of available PRBs and the lowest shows the resulting throughput. . . . .	37
4.11	Power savings from the ECO-mode in a radio C. The graphs shows scenarios with and without Micro Sleep TX and LESS. . . . .	38
4.12	A random generated load profile based on equation 4.9 and inspired by data from a real suburban RBS. The graph shows a 24 h scenario starting from midnight. . . . .	41
4.13	The upper graph shows the amount of available PRBs limited by the ECO-mode. The thresholds for switching off the ECO-mode are 50 for the last value, 60 for the predicted value and the ECO-mode has to be switched off for at least 5 hours. . . . .	42
4.14	Simulated values for the load and ECO-mode over 7 days. The ECO-mode is used in 62% of the time and PRB-usage is higher than the available PRBs for 30 minutes. . . . .	43

4.15	Load profile for the adaptive ECO-mode test. Three UEs are attached, each with 40 Mbps. They have different delays and duration to create a staircase formation. . . . .	45
4.16	Comparison of the power consumption with and without the ECO-mode in a radio B. Both tests have Micro Sleep TX and LESS activated. When the adaptive ECO-mode is used the ECO-mode is turned on from the start. When reaching 80 Mbps it's turned off after 36 seconds and is remaining in that state for the highest load. When the load is coming back to 40 Mbps the ECO-mode is turned on after 39 seconds. The thresholds are set to 50 and 57 used PRBs for current and predicted value. . . . .	46
4.17	The load profile used to test the adaptive ECO-mode for radio C. The throughput is varied with the amount of UEs that are attached where each UE is using 1 Mbps. . . . .	47
4.18	Comparison of power consumption with and without the adaptive ECO-mode. Both tests have Micro Sleep TX and LESS activated. The thresholds for switching on the ECO-mode are set to 30 for both current and predicted PRB-utilization. . . . .	48
5.1	Solar insolation and Peak Sun Hours [17] . . . . .	53
5.2	Solar insolation data on horizontal and an optimally tilted surface at a particular location . . . . .	54
5.3	Global Horizontal Irradiation map . . . . .	55
5.4	Off-grid PV system block diagram . . . . .	56
5.5	Overall design of a solar powered RBS. . . . .	57
5.6	Average solar insolation on optimally tilted panel at two locations in Europe . . . . .	58
5.7	The mobile traffic pattern in urban, suburban and rural areas . . . . .	59
5.8	Energy demand by load . . . . .	67
5.9	Energy demand by load and battery with safety margin . . . . .	68
5.10	Energy demand by load and battery with annual average PSH . . . . .	69
5.11	Fully solar powered site set up . . . . .	71
5.12	Fully diesel powered site set up . . . . .	73
5.13	Solar diesel hybrid site set up . . . . .	75
5.14	Cost trend for a combined solar cell and diesel powered RBS in Kista. The RBS is assumed to use all power save features and has an energy consumption of 40 kWh per day . . . . .	76
5.15	Cost trend for a combined solar cell and diesel powered RBS in Lisbon. The RBS is assumed to use all power save features and has an energy consumption of 40 kWh per day . . . . .	76



---

## List of Tables

---

3.1	Power savings when using the adaptive fan script. The current fan algorithm means that the fan is set to 35%. . . . .	19
4.1	Power savings from ECO-mode and Micro Sleep TX respectively. . .	30
4.2	Power savings for radio B in percentage for various loads. It shows the impact of using all three power save features together. . . . .	40
4.3	Average power consumption for the two RUs with and without the adaptive ECO-mode. The last column shows the power saving for each RU. . . . .	48
5.1	Comparison of different Solar Cell types . . . . .	52
5.2	Power consumption of the radio unit at a RBS . . . . .	60
5.3	Total power consumption at a RBS . . . . .	60
5.4	Number of Battery modules . . . . .	61
5.5	Comparison of different Solar Batteries . . . . .	62
5.6	Maximum peak power and area of solar panel required for the different months of the year in Kista . . . . .	63
5.7	Maximum peak power and area of solar panel required for the different months of the year in Lisbon . . . . .	64
5.8	Comparison of costs in a solar powered base station with and without power save features, all values are given in American dollars. . . . .	72
5.9	Comparison of costs in a diesel powered base station with and without power save features, all values are given in American dollars. . . . .	74
5.10	Comparison of the different power options analysed in this section. .	77





# Introduction

---

## 1.1 Objectives and structure of report

The world is today facing a rapid growth in telecommunication forcing the industry to deliver more traffic to more users at higher speeds. This increase in data traffic will also mean that network is heavily loaded which will increase the power consumption. The result is increasing energy bills for the operators while the customers are not willing to pay more for the service. It is therefore of great importance to design the telecommunication network as energy efficient as possible. This will be addressed in the chapter 3 and 4 where two energy efficiency methods are presented. A high power consumption becomes an even larger problem in sites that are not connected to the electrical grid, this could be due to rough environment or an unreliable grid. Those sites are usually powered by a diesel generator causing high fuel costs, maintenance and green house gas emissions. This can be solved by using modern renewable energy sources. In chapter 5 the possibility and design of a base station powered with solar cells is evaluated. The thesis starts with two introductory chapters that explains the concepts and vocabulary used throughout the thesis. The first chapter explains important telecommunication concepts in general and 4G/LTE in particular. The second chapter will address the power consumption in the network and explain the energy efficiency methods that are already implemented.

## 1.2 Telecommunication

To wireless connect people all around the world radio waves are used. These are electromagnetic waves with frequencies ranging from tens of kHz up to the THz region. The waves are generated from a digital signal which sets parameters such as frequency, amplitude and phase. After the wave has been transmitted it

is received and the parameters of the analog radio wave is translated back into digital bits. To reduce interference between different base stations the operators transmits their data in certain frequency spectra, called bands. The width of this frequency range is called the bandwidth.

### 1.3 Radio Base Station

A Radio Base Station (RBS) consists of mainly three parts. The first one is the baseband, also called Digital Unit (DU). This handles the logic and processing, meaning that it decides which signals that should be transmitted to each user. The DU will then send the desired values through a optical fibre to the Radio Unit (RU) which uses fast Fourier transforms (FFT) to generate a radio wave. This wave is then transmitted from the antenna placed high up at the site. To increase the throughput, the amount of data it can transmit, the waves are divided into different polarizations [1]. This makes it possible to use the same frequency spectrum more efficient.

The RBS has been around for some time and has therefore faced a few different techniques. There is Global System for Mobile communications (GSM), Wideband Code Division Multiple Access (WCDMA) and Long Term Evolution (LTE). These are often referred to as 2G, 3G and 4G. In this master thesis our main focus is on LTE since it is predicted to become the most used technique in the following years as seen in figure 1.1. In this image the upcoming technique

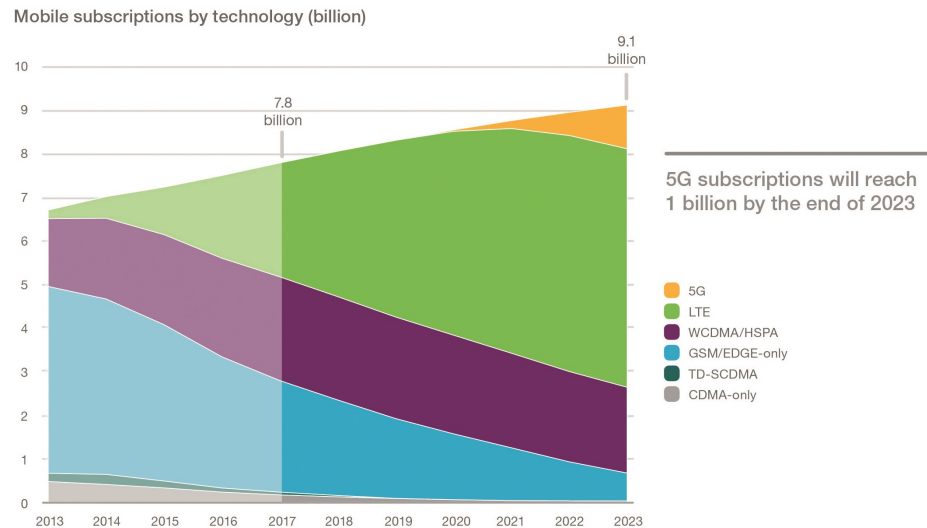


**Figure 1.1:** Mobile subscription per technology. The graph does not include Internet of Things (IoT) connections or Fixed Wireless Access (FWA) subscriptions [2].

New Radio (NR), referred to as 5G, is also included. Since it is expected take a few years before NR has a significant share of the subscriptions this is not investigated any further in this thesis.

## 1.4 Long Term Evolution

In LTE the bands have a bandwidth of 1.4 MHz to 20 MHz, to get a higher throughput it is preferred to have a large bandwidth. These bands are divided into 15 kHz subcarriers. A 20 MHz band is divided into 1200 subcarriers, meaning that some part of the bandwidth is not used. This is the guard band which is located at the edges and prevents different bands from overlapping. These subcarriers are organized together in groups of 12 which makes up 100 resource blocks in the frequency domain. This is visualized for a 1.4 MHz bandwidth in figure 1.2. When expanded in the time domain this results in a grid of symbols that can carry

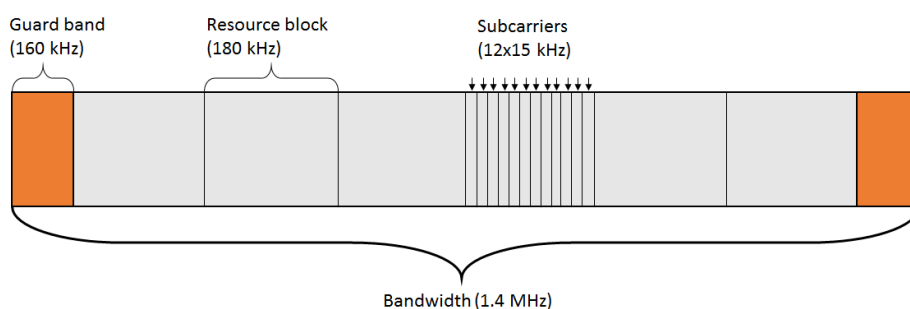


**Figure 1.2:** Schematic overview of the frequency domain for 1.4 MHz bandwidth. There are 6 resource blocks that consists of 12 subcarriers each and a guard band at both edges.

information. The smallest unit that can be scheduled is called Physical Resource Block (PRB). A PRB consists of 12 subcarriers in the frequency domain and 7 symbols in the time domain, they are then grouped in pairs that results in 14 symbols. These 14 symbols are evenly spread out in a Transmission Time Interval (TTI) of 1 ms where each symbol is  $71.4 \mu\text{s}$ . An example of a resource grid for a 1.4 MHz bandwidth is seen in figure 1.3.

### 1.4.1 Modulation

The throughput is dependent both the amount of symbols and how many bits that can be sent in each symbol. The number of symbols that are sent is dependent on the bandwidth as explained but the amount of bits in each symbols depends on the modulation that is used. The modulation of the signal decides how fine tuned amplitude and phase can be to obtain different values within a symbol. The

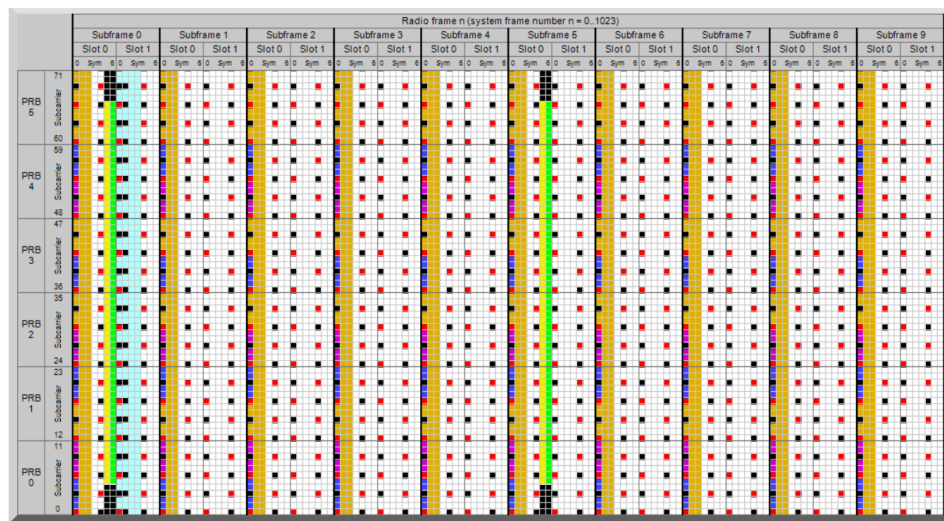


**Figure 1.3:** The resource grid for a 1.4 MHz bandwidth spanning over 10 subframes. There are 6 resource blocks in the frequency domain that all consists of 12 subcarriers of 15 kHz each. In time domain there are 10 TTIs all consisting of 14 symbols. These builds up the physical resource blocks that consists of 12 subcarriers and 14 symbols. There are coloured symbols in all PRBs, these are reference signals that will be explained later on. The image is generated through [3]

most simple modulation is Binary Phase Shift Keying (BPSK). This consists of two values with the same amplitude and a  $180^\circ$  phase shift in the complex plane. A symbol with a BPSK modulation can therefore differentiate between two values which is equivalent of one bit. The next modulation is the Quadrature PSK where 4 values are placed with the same amplitude and  $90^\circ$  phase shift, this results in two bits per symbol. In higher modulations called Quadrature Amplitude Modulation (QAM) both the phase and amplitude are used. When using 16-QAM a grid of 16 dots in the complex plane is used to send 4 bits per symbol. Examples of modulation schemes can be seen in figure 1.4

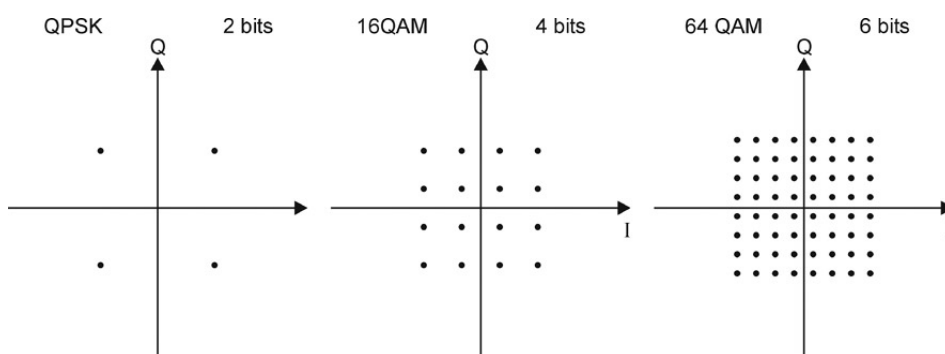


**Figure 1.4:** Modulation scheme for QPSK, 16-QAM and 64-QAM.

The angle and absolute value of the points corresponds to phase and amplitude of the wave [4].

It is often desired to have a large throughput which is acquired by using the highest modulation. But a high modulation requires that the transmitted signal is more accurate since the dots are closer together. This is expressed through the Error Vector Magnitude (EVM) that expresses how far from the desired point the received signal is. A high modulation will then need a lower EVM since the points are closer together [5]. When the signal strength is low it is therefore impossible to maintain a high modulation. The modulation is then reduced and the data is divided into a larger amount of symbols.

### 1.4.2 MIMO

As mentioned earlier the throughput of modern telecommunication is increased by using more than one polarization of the transmitted radio wave. This technique is referred to a Multiple Input Multiple Output (MIMO) transmission mode. Since the same frequencies are used several times the spectral efficiency is increased. The signals are transmitted from several antennas and are then received in several receiver antennas. Some rather complex signal processing are then used at the receiver end to translate the signal into digital bits.

### 1.4.3 Carrier Aggregation

Another method to increase the throughput is to use Carrier Aggregation (CA). This means that a base station can serve a single User Equipment (UE) with several carriers. The throughput is proportional to the number of carriers and the required data can be transferred faster. An example would be that 3 carriers of 20 MHz is used to triple the throughput. This is increasing the spectral efficiency as the data has more possibilities regarding where it is transmitted leading to that it is less sensitive to be delayed from data transmission to other UEs [6]. To be able to use carrier aggregation the operator has to buy more bandwidth.

### 1.4.4 Beam Forming

When transmitting a signal it is desired to have a large signal strength to the receiver without having to increase the output power from the base station. This is done by using the constructive and destructive interference of several closely spaced antennas in a method called beam forming. By changing the amplitude and phase of the antennas the sum of the waves can be added constructive in the desired direction. This means that the amplitude of the signal is directed towards the UE instead of being spread out in all directions. If more antennas are used the beam can be more narrow [7]. A well directed beam can deliver a large signal strength to the UE and reduce the interference with other signals.

### 1.4.5 Throughput

To calculate the throughput of an RBS running LTE a lot of factors have to be taking into account. These are bandwidth, modulation, diversity mode and the number of carriers. The throughput is then calculated through equation 1.1 where  $RB$  is the amount of resource blocks in the frequency domain set by the bandwidth,  $Mod$  is the number of bits per symbol,  $DM$  is the diversity mode that gives the number of polarizations and  $CA$  is the number of carriers through carrier aggregation.

$$\text{Throughput} = 14000 \cdot 12 \cdot 0.75 \cdot RB \cdot Mod \cdot DM \cdot CA \quad (1.1)$$

In the equation one can also see some numbers; 14000 is the amount of symbols per second, 12 is the amount of subcarriers per resource block and 0.75 comes from the fact that 25% of the symbols are used for control channels where no user data can be scheduled.

The result of equation 1.1 can be visualized with an example. If an RBS has a 10 MHz bandwidth with 10% guard band the available spectrum is  $10 \cdot 0.9 = 9$  MHz. Each subcarrier is 15 kHz and since a resource block consists of 12 subcarriers the

amount of resource blocks is  $RB = 9000/(15 \cdot 12) = 50$ . Further on assuming a 64-QAM modulation each symbol can carry 6 bits of information, giving  $Mod = 6$ . If the diversity mode is 2x2MIMO the radio is transmitting in two polarizations giving  $DM = 2$ . Last, if there are 2 possible carriers, the carrier aggregation gives  $CA = 2$ . The result of these numbers is seen in equation 1.2

$$\text{Throughput} = 14000 \cdot 12 \cdot 0.75 \cdot 50 \cdot 6 \cdot 2 \cdot 2 = 151.6 \text{ Mbps} \quad (1.2)$$

It should be noted here that this is a theoretical maxima that sets the limit for the performance of a base station. In real situations the noise has a heavy impact on the throughput since it forces a lower modulation to maintain an acceptable SNR. The achieved throughput is also lowered as some data never reaches the receiver due to path loss in buildings, cars or other obstacles.

#### 1.4.6 Idle mode

When there are no connected UEs at a base station it is in idle mode. This means that data towards a UE is transmitted neither through uplink nor downlink. However, the RBS is still showing its availability through Cell specific Reference Signals (CRS). These are located in a specific pattern within each PRB as seen in figure 1.5. This means that the RBS is transmitting some symbols even when no UEs are attached.

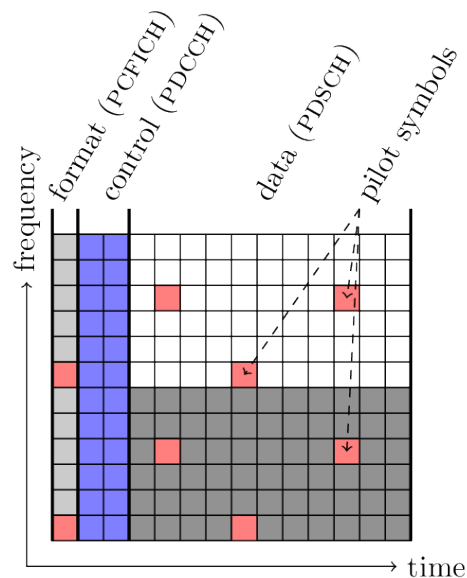


**Figure 1.5:** A PRB with no scheduled data. Image taken from [8].





## Energy Consumption

---

Around the world there are 5 million RBS all together consuming around 2% of the worlds total electrical energy consumption [9]. More than half a million of these RBS requires off-grid power supplies due to either a non-reliable electrical grid or a location which makes a grid connection impossible [10]. These base stations are then powered with diesel generators that generates both Green House Gas (GHG) emissions and pollution in the nearby area. It is also expensive for the operator to provide the RBS with diesel. This makes it important to try to construct the RBS as energy efficient as possible. If the power consumption is lowered the possibility of using renewable energy sources such as solar power becomes larger. This will be discussed further in the thesis.

One of the main problems with the consumption in the base stations is that it doesn't scale very good with the load. This means that even at very low load the power consumption could be almost 50% of what it is at maximum load. This is a problem since the vast majority of RBS are at low load at most times. An example of the power consumption in RU is seen in figure 2.1.

The load varies over the day meaning that in most base stations there is a higher load during the day than during the night [11]. This means that the power consumption will most often be higher at day time. For an off-grid site powered with solar energy this is an advantage since all the power will be produced during daytime. If the curves of produced and consumed power are following each other the need for battery capacity becomes less and the price for installation is reduced.

### 2.1 Energy Efficiency Methods

A common approach when it comes to reduce the power consumption is to look at what happens at low load. The goal with these kind of methods is to make the power consumption scale better with the load. This will make the RBS go from

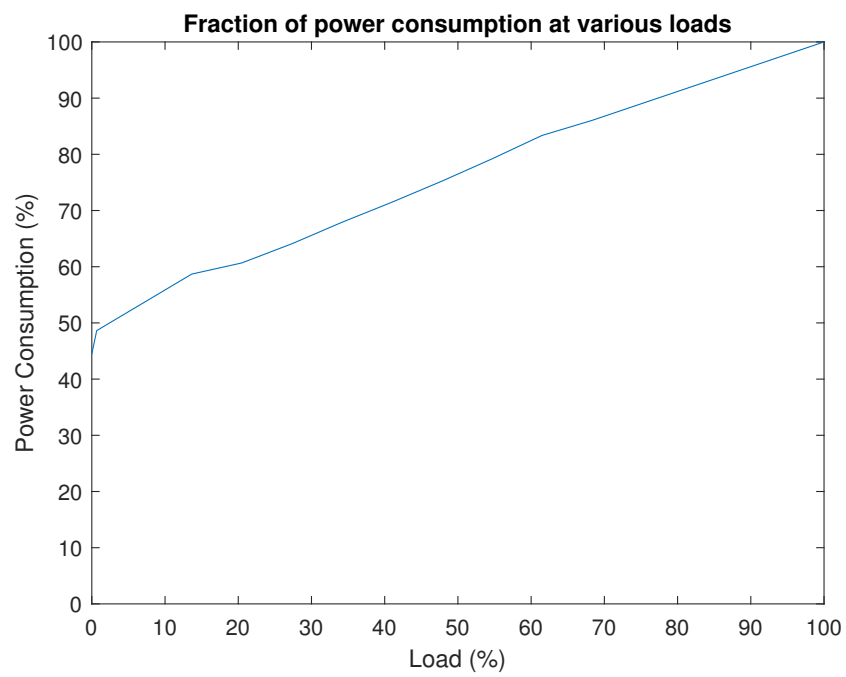


**Figure 2.1:** The power consumption at various loads for a typical RU. The load and power consumption are measured in percentage of their maxima. Measurements performed in the lab at Ericsson Lund.

an 'always-on' to an 'always-ready' state.

### 2.1.1 Psi-Omni

The most common configuration of a base station is to use one Radio Unit (RU) for each antenna. All of these RUs are consuming large amounts of power that could be unnecessary regarding the required capacity. In areas with a low load demand a single RU can connect three antennas. This configuration looks similar to the Greek letter  $\Psi$ , thus the name. Fewer RUs will reduce the total power consumption of the base station at a cost of a lower maximum throughput.

### 2.1.2 MIMO Sleep

To increase the throughput a Multiple Input Multiple Output (MIMO) transmission mode is used. This means that data is transferred in two different polarizations. During low loads this might not be necessary and one of the TX branches can be turned off. This results in a lower power consumption. The price for turning off one polarization is that less data can be transmitted. In a high load scenario this means that the throughput is lowered. If the load is low the two polarizations are transmitting the same symbols to increase robustness and coverage that will increase the cell size, this is referred to as diversity. Activating MIMO sleep might then interfere with this.

### 2.1.3 Micro Sleep TX

The component that is accountable for the single largest portion of the power consumption is the Power Amplifier (PA) in the RU [12]. This amplifies the signal in the RU so it can be transmitted. In a regular case the PA is turned on at all times independent of the load. When Micro Sleep TX is used the PA turns off every-time it faces a symbol in the time domain which is empty. This means that when a PRB only consists of CRS signals the PA is switched off during a majority of the time resulting in drastic power savings without reducing the capacity. Looking at the PRB in figure 1.5 one can see that 4 of 14 symbols in time domain have CRS symbols meaning that they require the PA to be turned on. There are also other signals such as Physical Downlink Control Channel (PDCCH) that limits the use of Micro Sleep TX. This results in that Micro Sleep TX can be used in 8-9 of 14 symbols in time domain. The PA will also need to be turned on a few  $\mu s$  in advance since it has short ramp-up time.

### 2.1.4 LESS

Micro Sleep TX can only switch off the PA when all PRBs are empty in the frequency domain. It is therefore favourable to spread out the data in the frequency domain rather than the time domain to leave more empty PRBs where Micro Sleep TX can work. This is done with the Low Energy Scheduler Solution (LESS). This means that data with a low priority is not transmitted instantly. It is instead buffered until either the LTE grid is filled to a threshold in the frequency domain or a high priority data packet has to be sent. This will introduce low but acceptable delays in the low priority data and will allow Micro Sleep TX to work more efficient also at higher loads. It is not affecting the average throughput.

### 2.1.5 Ericsson Lean Carrier

The Ericsson Lean Carrier (ELC) is a method to adjust the bandwidth that the CRS is transmitted in. If the RBS is only transmitting CRS signalling it is unnecessary to use the entire bandwidth since no actual data is transmitted. This gives the possibility to reduce it to a more narrow band in the middle of the bandwidth. The result is a lower output power compared to when the entire bandwidth is used.

### 2.1.6 Gallium Nitride transistors

Traditionally electrical components are built with Silicon as the semiconductor material. However, in newer technology some other semiconductors are being used such as Gallium Nitride (GaN). The larger bandgap in GaN compared to Si makes it possible to make the device smaller while still maintain an electric field that is strong enough. A smaller device results in a lower on-resistance which improves the power efficiency of the transistor [13]. This means that less power is lost in the conversion. The larger bandgap is also making GaN devices less sensitive to high temperatures since the thermal energy of the electrons is significantly lower than the bandgap, this means that thermal leakage becomes less of a problem. Another property of the GaN transistor is that it has an optimal operating point for power efficiency. This means that it can be designed more power efficient if the biasing level is known beforehand.

### 2.1.7 Predicting data

A lot of the power saving features are designed for scenarios with low load. This is the reality for most base stations at most times. But it is important that a power save mode can be switched off quickly when the load is increased. It is hard to predict the load at a particular RBS since it can have sudden peaks. At these peaks the users would still demand their data transfer with a negligible delay. This means

that in order for an operator to use a power save feature that reduces throughput it is crucial that the throughput can be restored when needed. These changes can happen in the time range of milliseconds which means that this is roughly how fast the mode has to turn off. When switching between certain modes it might introduce some downtime in the system. It is therefore not desirable to switch too often. This could be controlled by using parameters such as PRB utilization or amount of buffered data as inputs in a time series analysis.

## 2.2 New methods

In this thesis two new energy efficiency methods are presented. The first one is for the baseband and addresses the problem with wasted power due to thermal leakage in the circuits. In high temperatures this effects gets larger and the base station consumes more power. To lower the power consumption a new method is applied to control the fan that cools the baseband. This is an example of a method that saves power without affecting the performance and can be run continuously independent of outside factors. The second feature is focusing on the RU and uses the ability to lower the PA biasing by restricting the available resource blocks. This method is suitable for times and locations where the load is low since it will save power by limiting the throughput.



## Baseband cooling

---

Some of the measured values in this chapter are presented in arbitrary units (a.u.) in order to protect confidentiality. This is done through an individual scaling factor for each figure, meaning that that relative comparisons within a figure are still valid.

### 3.1 Background

The baseband, or DU, is the digital part that handles the processing of the base station. It contains EMCAs (Ericsson Multi Core Architecture) which can be configured to run either WCDMA, GSM, LTE or a combination depending on the needs at the location [14]. This baseband is placed in a cabinet often located at the bottom of the base station. However, this is not an isolated environment and the ambient temperature changes will also change the temperature in the baseband itself. As in many circuits the risk of overheating is mitigated by placing fans at one edge that circulates the air and thus lowers the temperature.

Except from the risk of overheating in the baseband there is also another problem regarding the temperature. As the temperature of the baseband is increased the thermal energy of the electrons in the ASICs is increased. This means that the components have to be biased at a higher level to compensate. Since the power consumption is proportional to the square of the voltage level a higher biasing leads to an increase in the power consumption. This suggests that a high fan speed could be good in terms of energy efficiency.

## 3.2 Fan Power Consumption

When measuring the power consumption of the baseband one will also have to include the consumption of the fan itself. The control parameter of the fan is the fan speed measured in percentage of its maximum. Since it is a rotational motion the required kinetic energy is given as equation 3.1

$$E_{rot} = \frac{I\omega^2}{2} \quad (3.1)$$

where  $I$  is the moment of inertia and  $\omega$  is the angular velocity. This means that the power consumption is proportional to the square of the fan speed. To support this theory a test was done by measuring the fan power consumption at various fan speeds. The result of this is seen in figure 3.1. The conclusion that can be

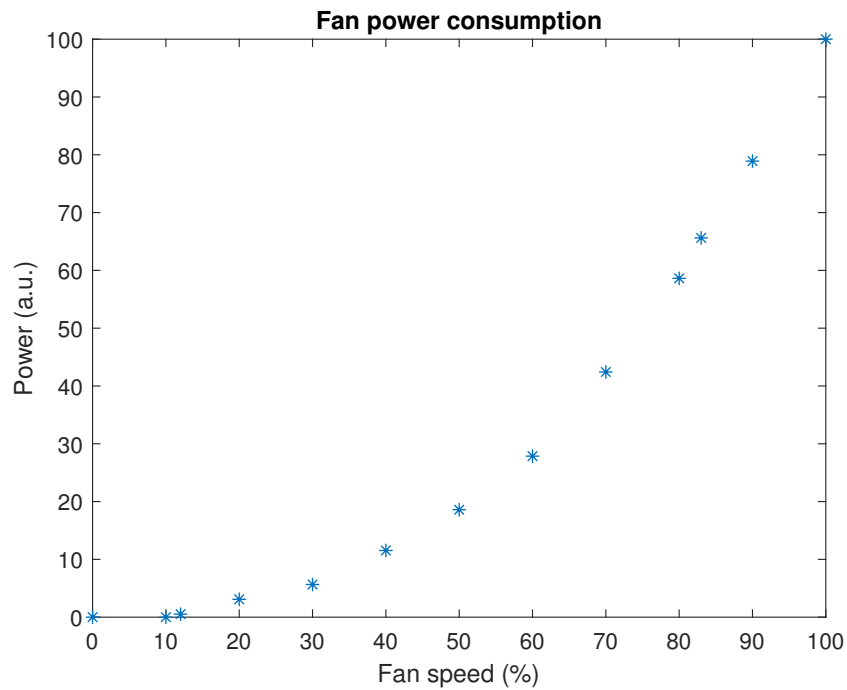


**Figure 3.1:** The power consumption of the fan at different fan speeds.

made from this result is that if the fan speed is too high the reduction in power consumption from the cooling effect could be smaller than the increase in the power consumption of the fan itself.



### 3.3 Optimal fan speed

Since the total power consumption, meaning both baseband and fan, will increase at both high and low fan speeds our theory was that there should be a fan speed where the power consumption is at its lowest. To test this the total power consumption was measured for various fan speeds. These measurements were done for 6630 baseband in a climate chamber and were repeated for different ambient temperatures. The result is seen in figure 3.2. There are a few conclusions to be

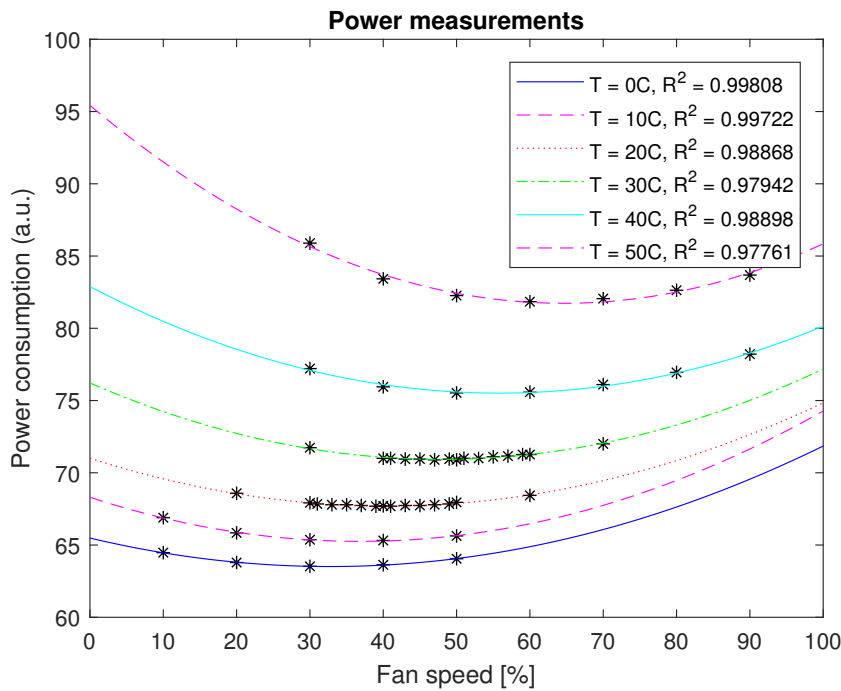


**Figure 3.2:** Total power consumption measured for various fan speeds at different ambient temperatures. The lines are fitted second order polynomials and their corresponding  $R^2$ -values are shown in the upper right box.

made here. First of all the measurements supports our theory that there is an optimal fan speed for the lowest power consumption. How large this fan speed should be increased with increasing ambient temperature.

## 3.4 Adaptive fan speed

Out on the sites where the baseband is located the conditions have a large variety both in terms of ambient temperature, work load and isolation in the cabinet. It would therefore be very challenging to write an equation for the optimal fan speed that captures all of these parameters in a good way. Instead we chose a method where the power consumption was measured continuously and the fan then adjusts itself in small steps to achieve the lowest power consumption.

When testing this method we faced some challenges. The first one was that the temperature changes and thus the changes in power consumption is a very slow process and it takes a long time for the measured value to stabilize after changing the fan speed. This was solved by doing a linear regression of four measured values and then looking at the slope of the resulting curve. If the absolute value of the slope is sufficiently small the power is considered to be stable. To catch quick variations in the power consumption all of these four measurements were taken from a ten point average.

Another problem was that the variation in the power consumption is rather large, this means that a small change in fan speed towards the optimal value still has a high risk of resulting in a higher power consumption. The fan will then take steps in the 'wrong' direction, away from its optimal value. With a larger step, from 1% to 3%, the effect of this issue was reduced a lot. Taking a larger step size will make it less precise when finding the optimal value. But looking at figure 3.2 the power consumption has a very small change in a 10% range around its minimum, meaning that the larger step size is not causing a major problem. When running the script it was also clear that it was easier for it to reduce the speed than to increase it. This is due to that a sudden increase in the fan speed will also increase the instantaneous power consumption and it will require some time before the cooling effect has reduced the leakage. A larger increasing step of 5% was introduced to even this out.

### 3.4.1 Safety features

The main reason why the fan is installed on the baseband in the first place is to prevent the components on the circuit board from overheating. In order to keep this a safety script was written. This script takes temperature measurements on certain parts of the baseband and compares these to threshold values set by the user. If some part of the baseband is too hot the fan speed is set to its maximum. This safety script is continuously running to be able to catch quick variations. However, to prevent the baseband from getting close to this threshold value another safety feature was added. This catches the case when the fan speed is too low for the power to stabilize. If the linear regression detects 6 positive slopes the power is assumed to not be stabilizing and the fan speed is increased by 10% to prevent the baseband from getting close to overheating.

### 3.5 Test method

To visualize the result of this adaptive method some test were done. A 6630 baseband was put in the climate chamber connected to one radio and only transmitting CRS signals. The initial fan speed was set to 35% to imitate the current solution. Our script was then running until the fan speed and power consumption reached a steady state. Since the fan will change up and down around its optimal value four subsequent measurements were averaged. This test was done for the ambient temperatures of 30°C, 40°C and 50°C. These temperatures were chosen since the power save is most significant for locations with high temperatures.

### 3.6 Results and comments

The current fan control sets the fan to 35% as a default and will then only increase if there is a risk of overheating. As seen in figure 3.2 this is close to the optimal fan speed at lower temperatures but as the temperature increases the difference gets larger. This is seen in figure 3.3 where the baseband power consumptions at an optimal fan speed and at 35% are compared. These values are taken from figure 3.2 and sets a maximum for the power savings. The power savings obtained from the adaptive fan are presented in table 3.1.

Temperature (°C)	Current (a.u.)	New (a.u.)	Savings
30	100	99.07	0.93%
40	100	99.12	0.88%
50	100	98.19	1.81%

**Table 3.1:** Power savings when using the adaptive fan script. The current fan algorithm means that the fan is set to 35%.

It is clear that the power savings are larger at higher temperatures meaning that this method would have a greater impact at base stations placed in a hot climate. These power savings can be expressed in saved money in the installation cost of solar cells. It will reduce the CAPEX of the RBS both in terms of reduced number of solar modules and battery size. It is fairly common that locations that are best suited for solar cells have high temperatures, meaning that this power save feature can have a large impact in those sites.

It is also crucial that the method is able to catch quick variations in temperature. This was tested by rapidly increase the temperature by 10°C and letting the script find the new optimal fan speed. It was seen that this took less than 60 min in all cases. This result is satisfactory since it is unlikely that the temperature would change more than 10°C within 60 min.

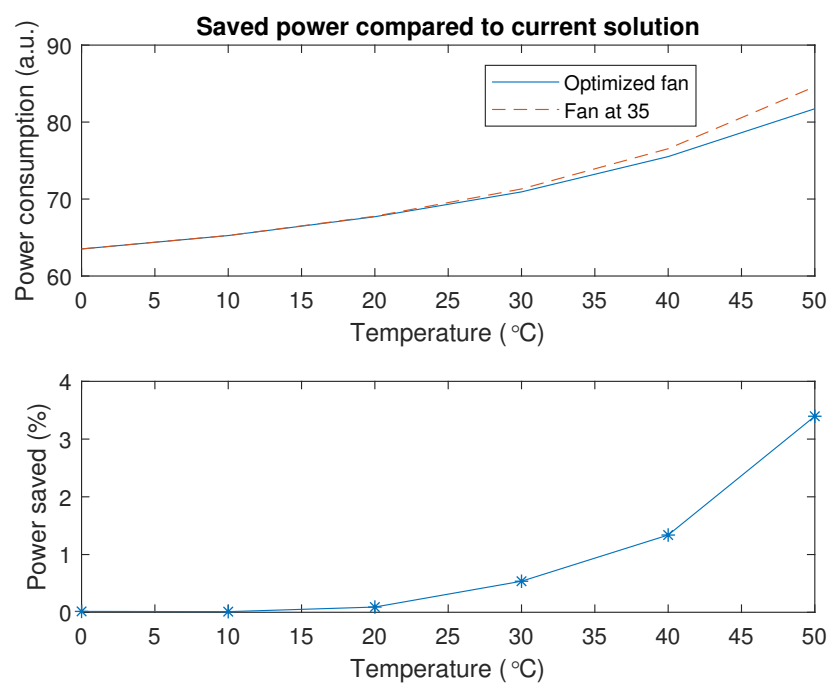


**Figure 3.3:** The graph at the top compares the power consumption of the baseband when the current fan control and the adaptive fan control methods are used. The difference between these graphs are then seen at the bottom.

### 3.7 Discussion

The method explained here is good in the way that it saves power without affecting the performance of the base station. It is more of an optimization of the current situation rather than a new feature. This means that it can run continuously in the baseband without having to be switched on and off. In that sense this energy saving is for free. However what would have to be investigated further before implementation is how the fan control would affect the lifetime of the fan, in a lot of cases this method is setting a higher fan value than before. Since maintenance is a large and unwanted expense for the operator it is important to secure that this will not lead to a shorter Mean Time Between Failure (MTBF). We have not been able to find any good study on this subject and it would be too time consuming to do an experiment within the thesis.

Another consequence of a higher average speed is that the temperature on the baseband is lowered. It is possible that this could increase the lifetime of the components on the board. Since maintenance on the board itself is more time consuming and expensive than changing a fan this would create a possibility that the total cost of maintenance could be reduced as well as the energy bill. So to summarize, this method can save energy but it needs more investigation on how it affects the MTBF. It is most effective in hot climates which corresponds quite well to where solar radiation is high meaning that it could work well in a solar powered base station.



## ECO-mode

---

Some of the measured values in this chapter are presented in arbitrary units (a.u.) in order to protect confidentiality. This is done through an individual scaling factor for each figure, meaning that that relative comparisons within a figure are still valid. The three radios used in this chapter will be referred to as A, B and C.

### 4.1 Background

When a base station is transmitting data in LTE the DU has the possibility to schedule all the resource blocks in frequency domain. This means that the PA in the RU has to be biased at a level corresponding to a full load scenario. But in most cases only a fraction of the PRBs are used meaning that the biasing of the PA and thus the power consumption is unnecessary high. The idea with an ECO-mode is that if one can ensure that not more than a certain amount of the PRBs are scheduled the biasing on the PA and thus the output power can be reduced. A schematic overview of this feature is shown in figure 4.1. Today there is a similar function which reduces the output power in order to protect the hardware in the RU from high temperatures. It will automatically do backoff if there is risk of overheating. This backoff resizes the PA and lowers the power consumption.

### 4.2 ECO-mode

Since this backoff is already implemented as a safety feature in the existing radios the idea is to trigger it with a low load level instead of a high temperature. It could then be ran as long as the load stays below a certain level. Since it is reducing the output power by not scheduling all PRBs the cell size is not affected. This



**Figure 4.1:** Overview of an example with 10 resource blocks in frequency domain. In normal operation all PAs are biased, showed as "On" in the image. With backoff to the right there is a limit on the number of biased PAs and some are unbiased, showed as "Off". In this example the throughput is limited to 70% of its original value. This backoff can be used as an ECO-mode.

means that the base station will still be able to reach users at the same distance. The ECO-mode will however affect the maximum throughput and it is therefore required that it can be switched off quickly in a high load scenario. The output power could be reduced by 2 dB which is a 37% reduction meaning that 63 PRBs are left. The total power consists of other components as well and will not be reduced with the same fraction but it is still expected to be rather significant.

### 4.3 Scheduling

It is important that this works together with the existing scheduler function also in the case when not all PRBs are allowed to be scheduled. The Low Energy Scheduler Solution (LESS) uses a large amount of resource blocks in the frequency domain to free up space in the time domain. This is still possible but there will be an upper limit of how many resource blocks that can be filled before the data is transmitted. There is a possibility that this will decrease the usage of Micro Sleep TX and therefore increase the on-time of the radio.

When Micro Sleep TX is applied in idle mode the power consumption is lower than its regular consumption. The reduction is due to that the PA is switched off at most symbols but it's limited since the radio is still required to transmit some signals such as CRS. How much power the radio consumes is then dependent on



how many TTIs that can be freed up. This power  $P$  is then calculated through

$$P = P_0(T + \mu(1 - T)) \quad (4.1)$$

where  $P_0$  is the power with no Micro Sleep TX,  $\mu$  is the reduction in power when the PA is off and  $T$  is the fraction of how many TTIs are scheduled, meaning that  $T = 0$  in idle mode. In a simple model we are assuming that LESS is able to delay all data until 100% of the resource blocks are filled in frequency domain before it transmits. For a 20 MHz bandwidth this means 100 resource blocks. The fraction of TTIs can then be calculated as

$$T = \frac{L}{100} \quad (4.2)$$

where  $L$  is the load calculated as the average amount of scheduled resource blocks per TTI. When backoff is applied the total amount of resource blocks that can be scheduled is reduced to  $S_b < 100$ . The total power is also reduced with a factor  $\alpha$  giving

$$P_{backoff} = \alpha P_0 \left( \frac{L}{S_b} + \mu \left( 1 - \frac{L}{S_b} \right) \right). \quad (4.3)$$

By combining equations 4.1, 4.2 and 4.3 one can set  $P = P_{backoff}$  to see at which load the ECO-mode will result in the same power consumption as when it is not used. Solving these equations for  $L$  will then give

$$L = \frac{(1 - \alpha)\mu}{(1 - \mu)(\alpha/S_b - 1/100)}. \quad (4.4)$$

Equation 4.4 is only valid as long as the load is not exceeding the reduced amount of resource blocks, meaning that  $L \leq S_b$ . In order for the ECO-mode to actually save power the reduced power factor  $\alpha$  has to be small enough.

## 4.4 Comparison of RUs

The ECO-mode will be evaluated in three different RUs; A, B and C. The radio A is special in the sense that it is using GaN-transistors which is expected to affect the behaviour of the power consumption. This is because the transistor will have an optimal working point where it is most efficient meaning that it is not certain that a lower biasing level will reduce the power consumption. The next RU, radio B, has four branches and is therefore able to run a 4x4 MIMO configuration. This means that it can have twice the throughput compared to A and C that only has two branches. However, in these following experiments the B RU is configured to only use two of its branches. The last RU is a C radio which is an RU with two branches but without the GaN-transistors. Another difference is that it is a 2x80 W RU meaning that it can have a larger coverage, but in these test cases it is configured as 2x40 W. These three radios have different power consumption but they are also different in the sense of how efficient the power save features are, both ECO-mode but also other such as Micro Sleep TX. The differences are investigated in this chapter.

## 4.5 Measurements in idle

To get a first impression of how the backoff is affecting the RUs some measurements of power consumption were performed while keeping the RU in idle mode. This means that no UEs are connected and the radio is only transmitting reference signals. In the setup the RU is connected to a Keysight 6705 that can measure the power consumption. It takes one measuring point every millisecond and the power consumption was then taken as an average over 60 seconds to get an accurate value. The backoff was then increased manually in steps of 0.1 dB and the power consumption was taken at each step.

### 4.5.1 Radio A

When increasing the backoff in idle mode for the radio A one can notice power savings both with and without Micro Sleep TX activated seen in figure 4.2. With Micro Sleep TX the backoff is reducing the power consumption with 2.2%. The power saving from Micro Sleep TX itself can be taken by comparing the graphs at no backoff. It is reduced with 14%, giving  $\alpha = 0.978$  and  $\mu = 0.86$ . The behaviours of the graphs in figure 4.2 are slightly different, with Micro Sleep TX activated there is saw-tooth behaviour which is not as present in the case without Micro Sleep TX.

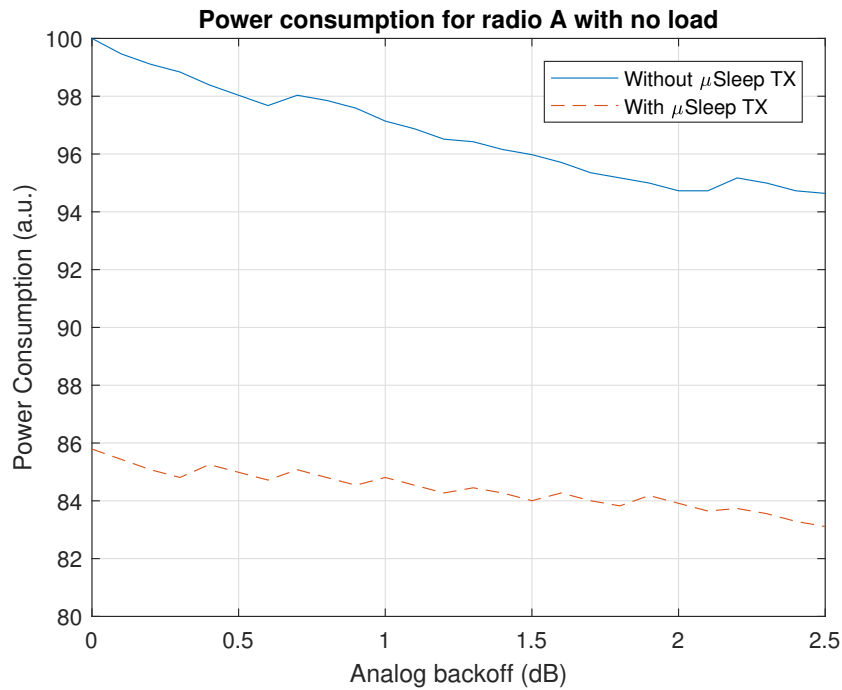


**Figure 4.2:** Power consumption for a radio A in idle mode and 40 W output power. The two graphs are showing the behaviour with and without Micro Sleep TX activated.

#### 4.5.2 Radio B

The result of the measurements with radio B is presented in figure 4.3. The behaviour of the power consumption when doing backoff is rather different from the radio A. There is no significant power saving at backoffs less than 1.9 dB but then one can see a large drop. A possible reason is that the analog backoff and the resizing of the PA is not actually happening at small backoffs, even though the radio reports an analog backoff. With Micro Sleep TX enabled one can see that the power consumption at 2 dB backoff is reduced by 3.8%. The power saving from Micro Sleep TX with no backoff is 14.4%, this means  $\alpha = 0.961$  and  $\mu = 0.86$ .

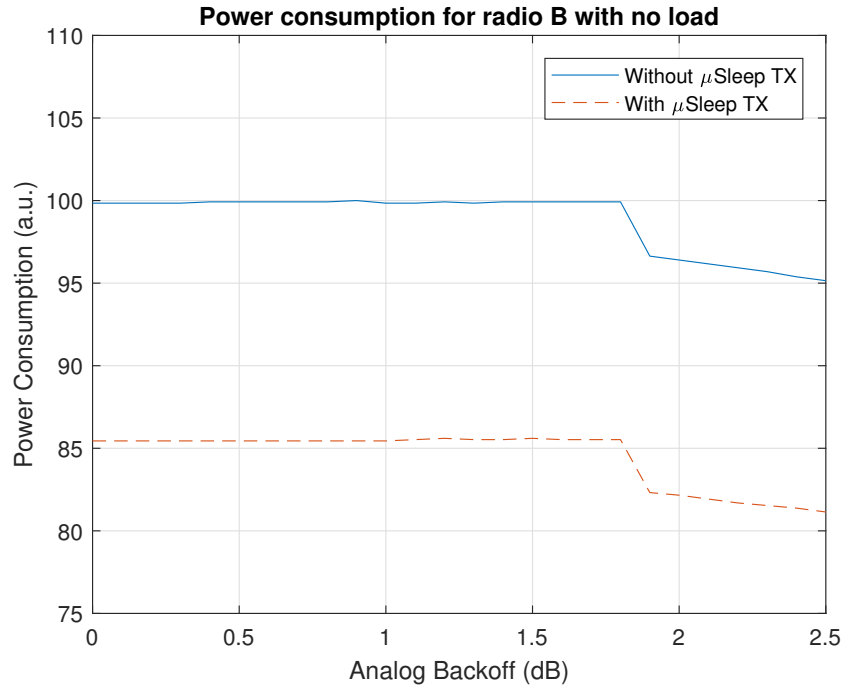


**Figure 4.3:** Power consumption for a radio B in idle mode and configured with 2 branches that has 40 W output power each. The two graphs are showing the behaviour with and without Micro Sleep TX activated.

### 4.5.3 Radio C

In the measurements with radio C in idle mode the behaviour of the backoff is similar to the radio A as seen in figure 4.4. A difference is though that the saw-tooth behaviour is not as significant resulting in a smoother curve. The power saving with Micro Sleep TX is 31% and the ECO-mode saves 3.7%, this gives  $\mu = 0.69$  and  $\alpha = 0.963$ .

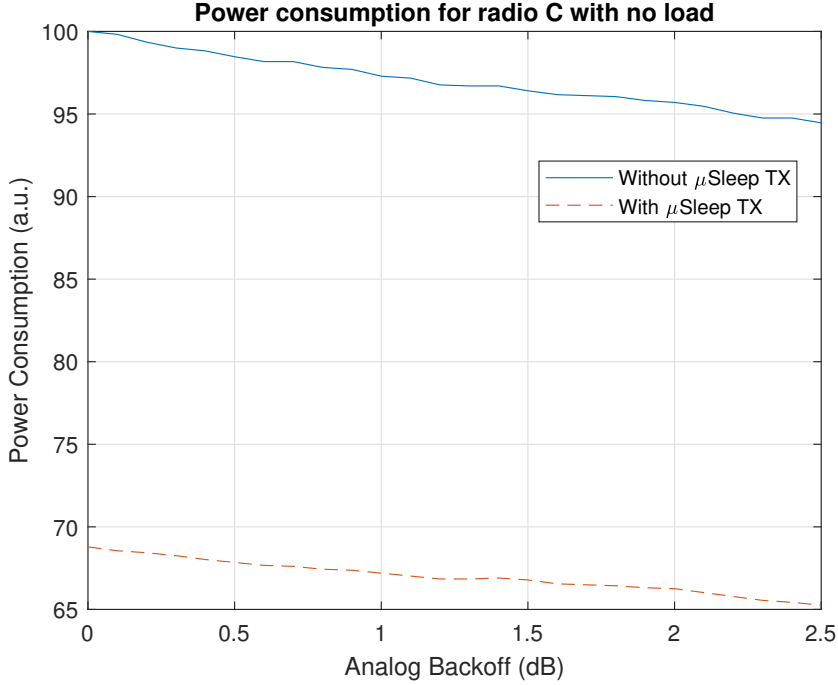


**Figure 4.4:** Power consumption for a radio C in idle mode and 40 W output power. The two graphs are showing the behaviour with and without Micro Sleep TX activated.

#### 4.5.4 Discussion

In the measurements with radio A, figure 4.2, one can notice a saw-tooth pattern in the graphs. Our first thought was that this has to do with the GaN-transistors which has an optimal operation point [13]. The reduced output power could therefore move the transistor from this point which is resulting in a higher power consumption. Another explanation could be found in the way that the backoff is implemented. But even though the behaviour is not fully understood the power savings in idle mode are still significant.

#### Max load

Looking back at the earlier reasoning about scheduling one can look back at equation 4.4 to see when the ECO-mode is effective. The values for  $\mu$  and  $\alpha$  are given from the measurements in idle mode, table 4.1, and the resulting maximal load can be seen in equations 4.5 to 4.7. In these cases the values are taken at a 2 dB backoff which gives 63 available PRBs, giving  $S_b = 63$ .

RU	$\mu$	$\alpha$
Radio A	0.86	0.978
Radio B	0.86	0.961
Radio C	0.69	0.963

**Table 4.1:** Power savings from ECO-mode and Micro Sleep TX respectively.

$$L_A = \frac{(1 - 0.978) \cdot 0.86}{(1 - 0.86)(0.978/63 - 1/100)} = 24.5 \quad (4.5)$$

$$L_B = \frac{(1 - 0.962) \cdot 0.86}{(1 - 0.86)(0.962/63 - 1/100)} = 42.9 \quad (4.6)$$

$$L_C = \frac{(1 - 0.963) \cdot 0.69}{(1 - 0.69)(0.963/63 - 1/100)} = 15.3 \quad (4.7)$$

It should be noted here, as discussed before, that LESS will not wait until all resource blocks are used. This means that the numbers here are lower than the actual values and can mostly be used to compare the different radios.

## 4.6 Measurements with load

After gaining knowledge about the behaviour in idle mode the next step is to see how the RUs behave when load is applied. This is done through a Viavi test equipment in which artificial load can be applied to the RUs. This can be specified with respect to the number of UEs, their total required throughput and their individual positions. In these measurements the UEs will be located in the center of the cell which will give them maximal modulation of 64 QAM, this is kept constant to make an easy comparison between throughput and PRB-utilization. The maximal throughput is obtained by using equation 1.1. All radios will be running a 20 MHz bandwidth, 64 QAM, 2x2 MIMO transmission mode and a single carrier. This result in the maximal throughput seen in equation 4.8.

$$\text{Throughput} = 14000 \cdot 12 \cdot 0.75 \cdot 100 \cdot 6 \cdot 2 \cdot 1 = 151.2 \text{ Mbps} \quad (4.8)$$

Two different measurements are done for each RU. First the maximal throughput is tested, the backoff is then increased in steps similar to the no load scenario. Here the effects of power consumption, available PRBs and throughput are measured. In the second measurement a 2 dB backoff is compared to the case with no backoff. This is done with and without Micro Sleep TX and LESS to see how these power save features affect each other. The values for each of the three radios are shown in the following sections and a discussion of the results can be found in section 4.6.4.

#### 4.6.1 Radio A

The result of the measurements with the radio A and 150 Mbps load is seen in figure 4.5. The three graphs are showing the power consumption, available PRBs and throughput. In figure 4.6 the resulting power consumption with a 2 dB backoff is shown.

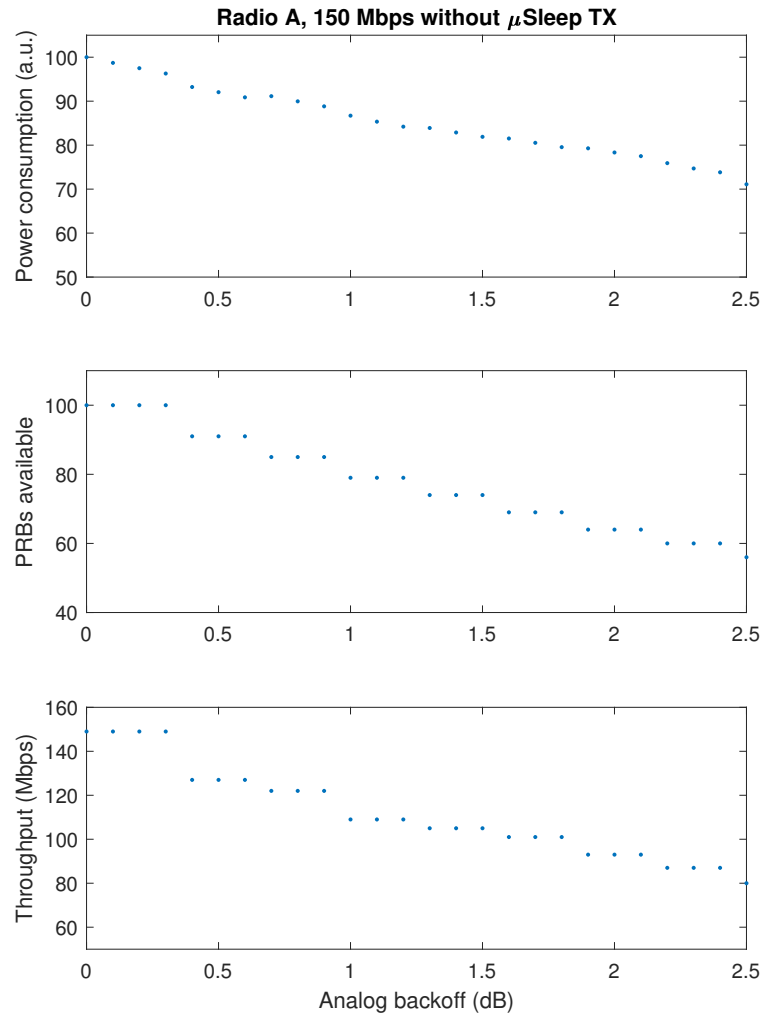


**Figure 4.5:** Measurements for a radio A with Micro Sleep TX deactivated. The backoff is increased from 0 to 2.5 dB in steps of 0.1 dB. The top graph shows the power consumption, the middle the number of available PRBs and the lowest shows the resulting throughput.



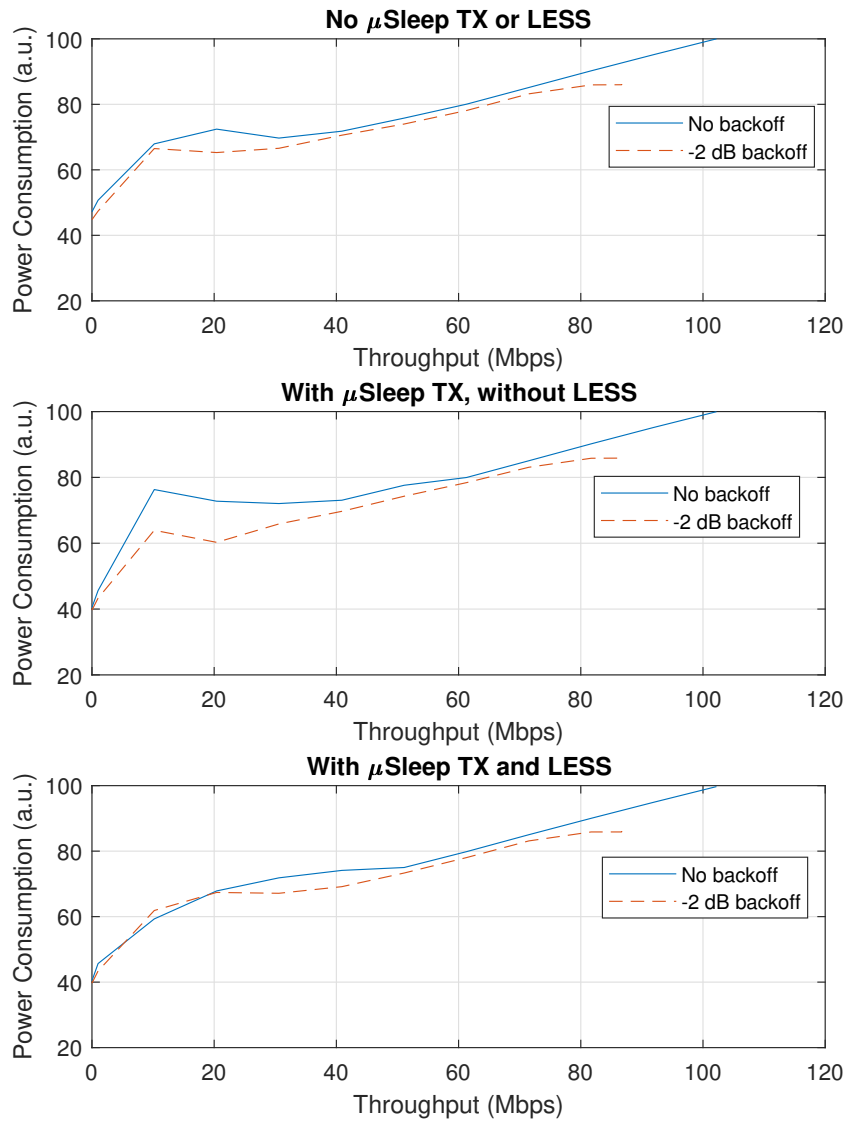


**Figure 4.6:** Power savings from the ECO-mode in a radio A. The graphs shows scenarios with and without Micro Sleep TX and LESS.

## 4.6.2 Radio B

When applying 150 Mbps load on the radio B the result in figure 4.7 was obtained.

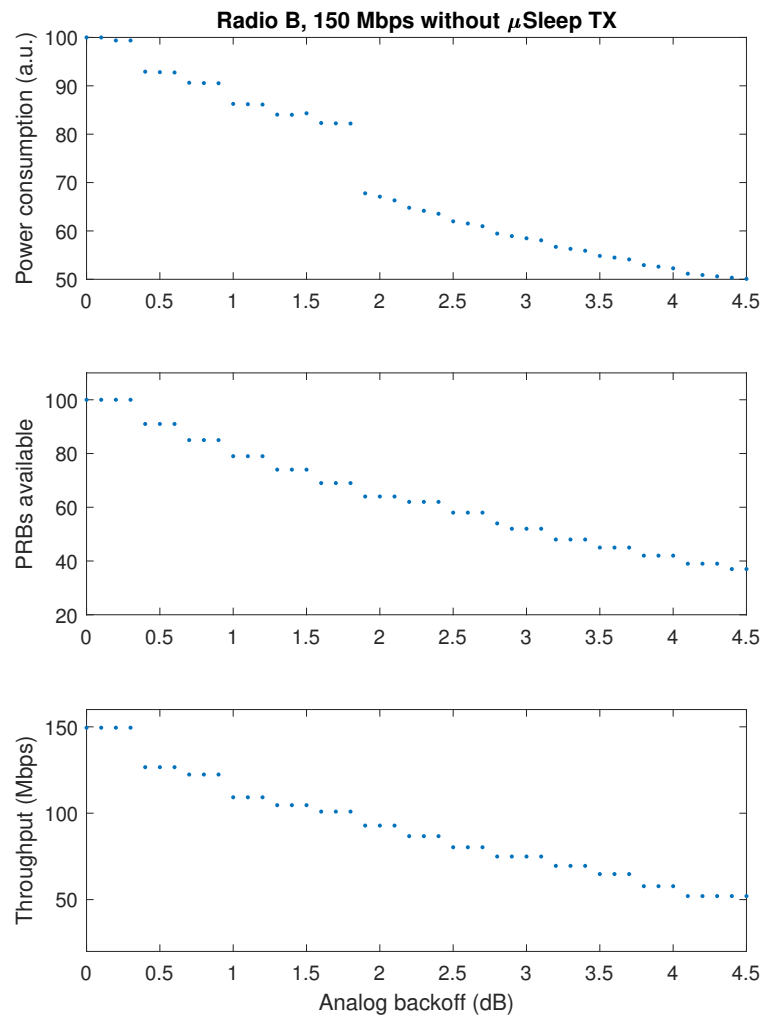


**Figure 4.7:** Measurements for a radio B with Micro Sleep TX deactivated. The backoff is increased from 0 to 4.5 dB in steps of 0.1 dB. The top graph shows the power consumption, the middle the number of available PRBs and the lowest shows the resulting throughput.

What one can now look at is the throughput per consumed power. That will tell us how efficiently the power is used. This is done by dividing the result from the top and bottom graphs in figure 4.7 and the result is seen in figure 4.8. It is desirable to use the power as efficient as possible which means that an analog backoff of 2 dB would be a good choice, that confirms that this is sufficient to use as an ECO-mode. The reason why this peak is there is the drastic drop in power consumption seen in figure 4.3 and the top graph of 4.7.

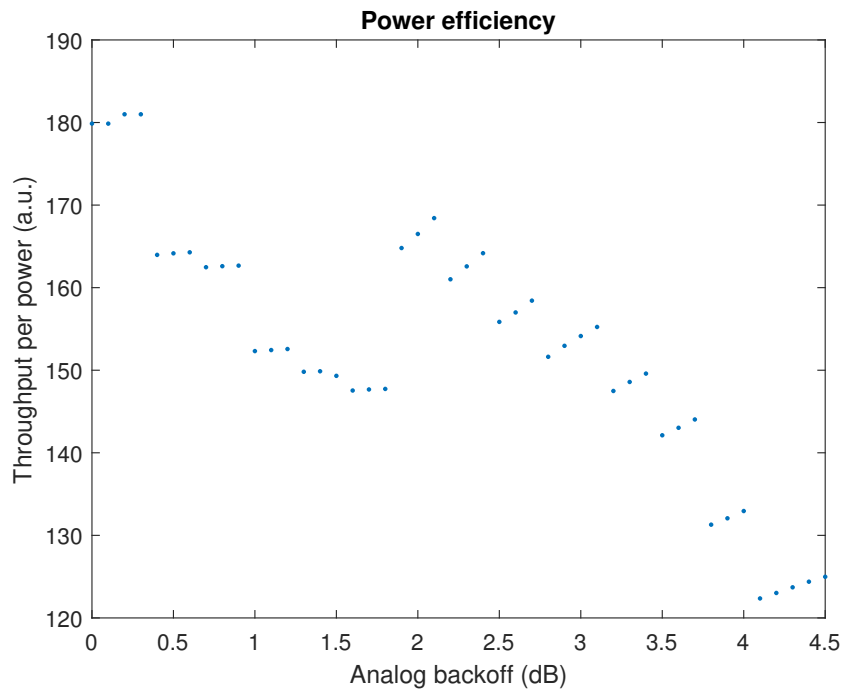


**Figure 4.8:** Measurements of the throughput per power for the radio B and for various analog backoffs. The graph shows the ratio between the top and the bottom graph of figure 4.7. The high ratio at -2 dB means that the power is used efficiently.

In the next measurement the power consumption was measured at various loads to see the effect of the ECO-mode seen in figure 4.9

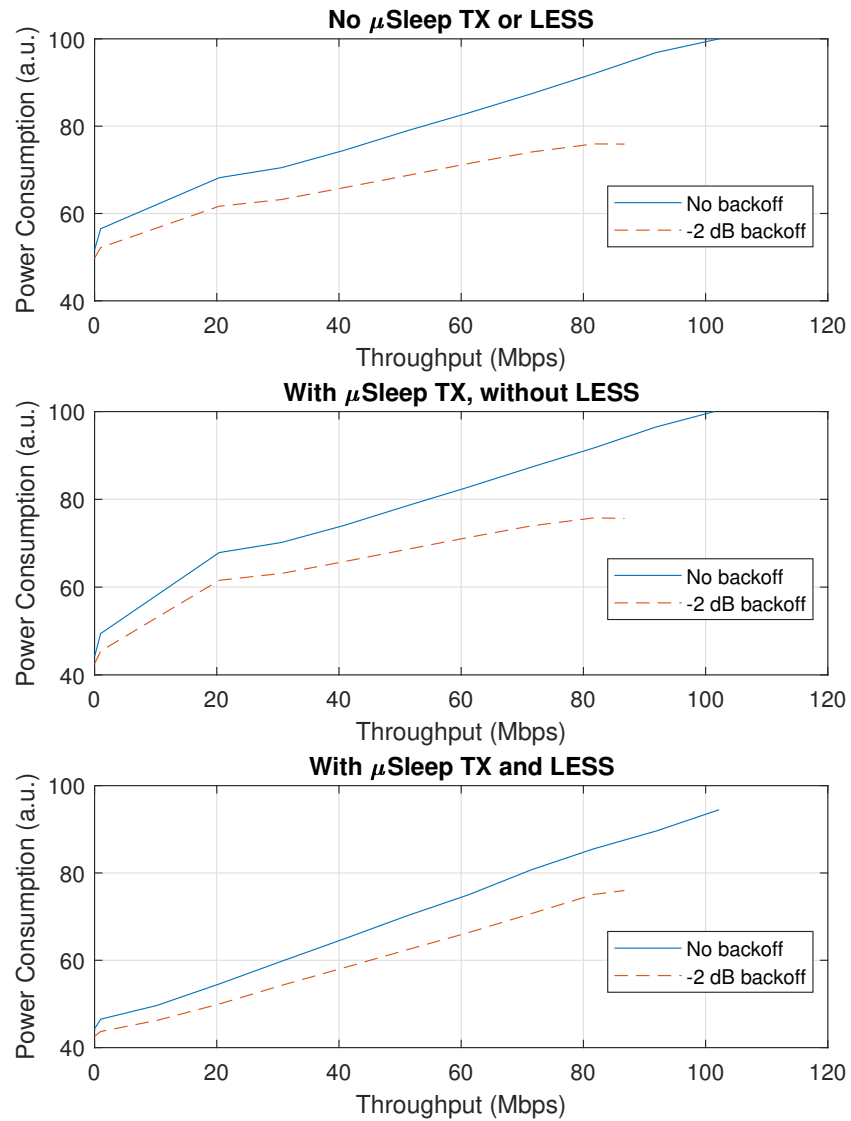


**Figure 4.9:** Power savings from the ECO-mode in a radio B. The graphs shows scenarios with and without Micro Sleep TX and LESS.

### 4.6.3 Radio C

The same measurements were done with radio C which gave the results seen in figures 4.10 and 4.11.

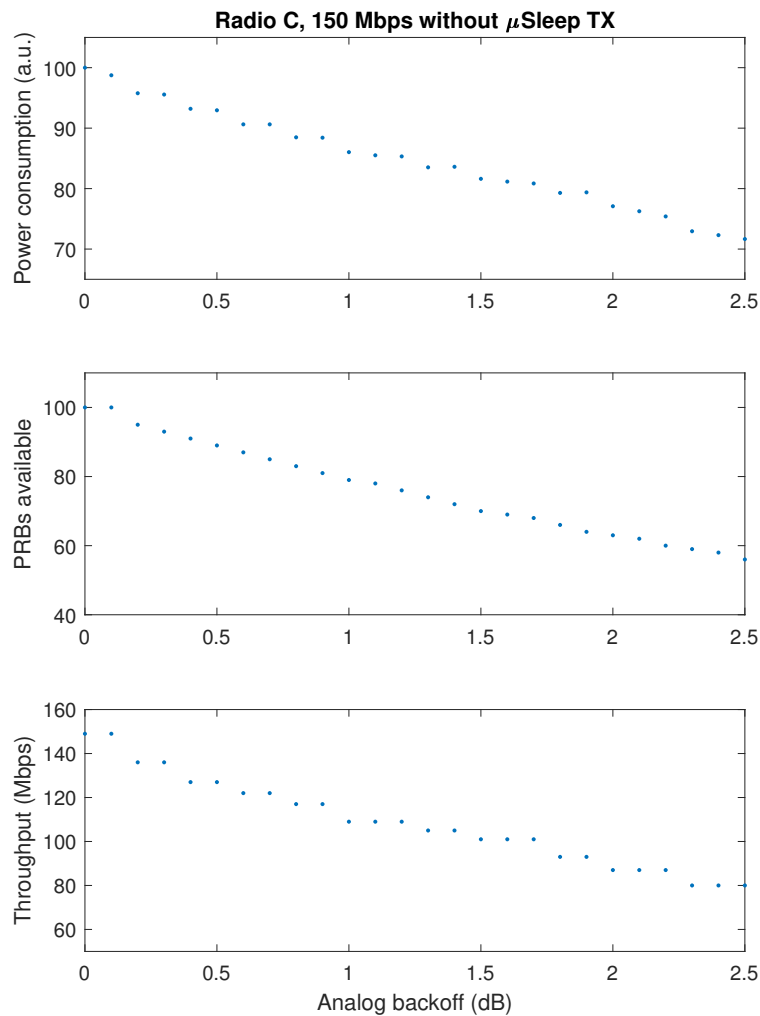


**Figure 4.10:** Measurements for a radio C with Micro Sleep TX deactivated. The backoff is increased from 0 to 2.5 dB in steps of 0.1 dB. The top graph shows the power consumption, the middle the number of available PRBs and the lowest shows the resulting throughput.

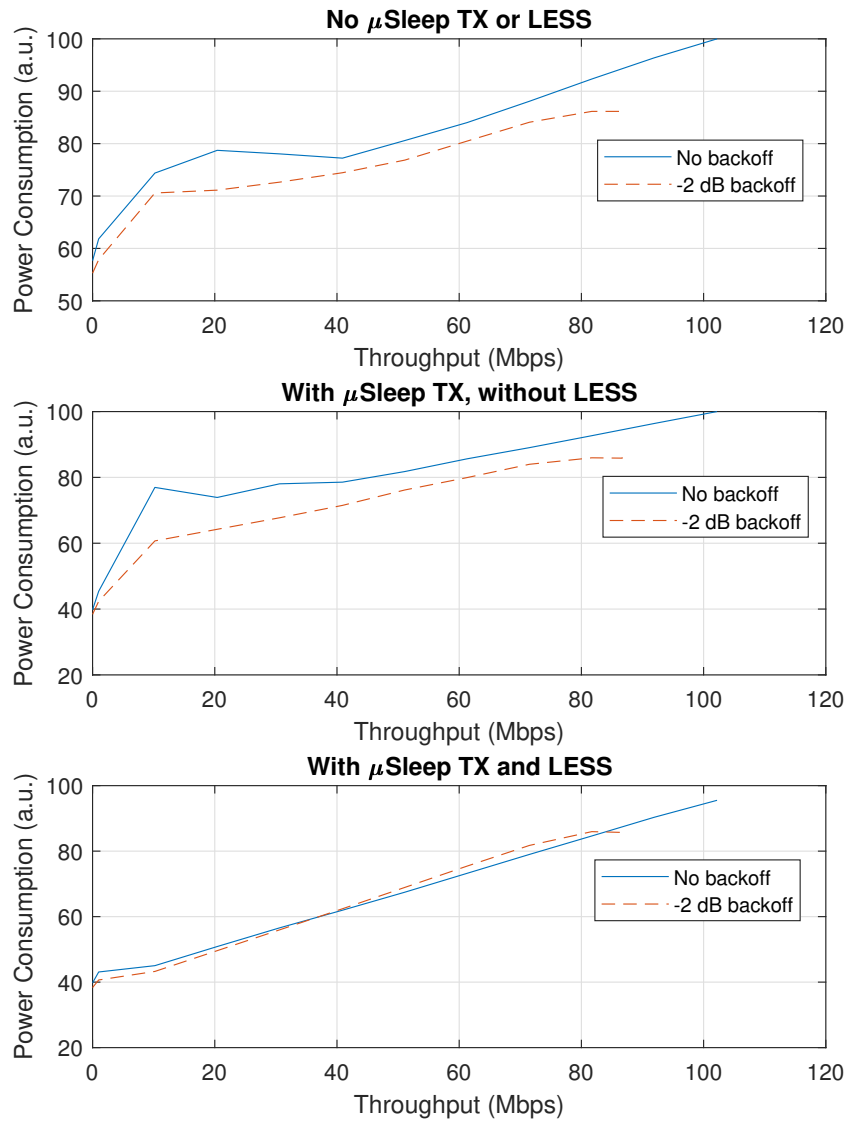


**Figure 4.11:** Power savings from the ECO-mode in a radio C. The graphs shows scenarios with and without Micro Sleep TX and LESS.

#### 4.6.4 Discussion

When running a high load the power consumption in the radio is increased compared to the idle mode. With increasing backoff the power is reduced but it will also reduce the throughput, just as expected. If one compares the two lower graphs of figures 4.5, 4.7 and 4.10 there are some similarities. As the amount of PRBs are reduced the throughput will also be lower. This result confirms that the backoff is re-sizing the PA by limiting the amount of available PRBs, meaning that it should not affect the cell size. The PRBs are then scheduled in groups of four which means that a small change in the available PRBs is not going to affect the throughput which can be seen for radio C in figure 4.10. The effect of the backoff is slightly different in the way that it is reducing the PRBs, but at 2 dB backoff all three RUs have 63 available PRBs. This means that the throughput will be decreased in the same way.

#### Power Saving

A first thing that is noticeable from figure 4.6, 4.9 and 4.11 is the cases with no backoff. These visualize how the previous developed features Micro Sleep TX and LESS work in practice. When comparing the two upper graphs one can see that Micro Sleep TX is most efficient at low loads. This is expected since it is dependent on that there are TTIs with no scheduled data which is hard to achieve at higher loads. However, when LESS is activated more TTIs are freed up and the data fills up in frequency domain instead. This makes Micro Sleep TX more efficient in higher loads and the power saving is significant even at 100 Mbps.

Further looking at the ECO-mode itself which is resulting in different power savings for the three radios. For radio A there is only a small power save in all three cases. It could have to do with how the backoff actually works and it would have to be investigated further. The power save seems to most significant for radio B and the bottom graph in figure 4.9 is probably the most important since an operator that is willing to save power is likely to already be using existing power save features. In this case the power saving is 3 to 13% depending on the load and without affecting the throughput. This suggests that it could be a good choice to use for an RBS that rarely uses its full potential. The resulting power saves in radio B for certain loads are given in table 4.2.

Load [Mbps]	$\mu$ Sleep TX, LESS & ECO-mode
0	17.6%
20	26.7%
40	21.7%
60	20.1%
80	18.4%

**Table 4.2:** Power savings for radio B in percentage for various loads. It shows the impact of using all three power save features together.

When comparing the ECO-mode with normal operation for radio C we can see that it saves power in the upper two graphs in figure 4.11, somewhat similar to radio B. But in the bottom graph with LESS activated the power consumption is actually higher for the ECO-mode when the load increases above 40 Mbps. To explain this we will look at the reasoning about scheduling earlier in this chapter. In equation 4.7 it was shown that this breakpoint would be at 15. An average PRB utilization of 15 per TTI corresponds to roughly 20 Mbps at 64 QAM. When looking at the bottom graph in figure 4.11 it seems like the lines intercept at 40 Mbps. The reason is as explained earlier that the model in equation 4.4 makes the assumption that LESS is always filling up all PRBs before transmitting which is not true. However, the result that this value of 15 is much lower than the maximum of 63 still suggest that the throughput where the ECO-mode increases the power consumption is lower than the maximum throughput.

## 4.7 Adaptive mode

In the last section it was shown that the ECO-mode can result in power savings for an RBS. The cost of this is that the maximal throughput is reduced. In a lot of base stations the throughput is rarely utilized to its full extent and it would therefore not be a problem to use this feature in the majority of the time. However, in these rare scenarios when the RBS has to transmit more data the ECO-mode has to be turned off.

### 4.7.1 Simulation

In order to find a reasonable model to try this on one has to estimate how the load profile looks like. This is very different for various base stations. Factors such as country or population density affects a lot. By looking at data from a typical base station in a suburban area in southern Europe the profile in equation 4.9 was assumed. This equation imitates the real values in a 24 h period, the load is



generally higher during the day but sudden increases can happen at any time.

$$\text{Load}(t) = 30 \left( 0.07(\epsilon(t)^3 + 1) \left( \left| \sin\left(\frac{\pi t}{96}\right) \right| + 0.2 \right) \right)^2 \quad (4.9)$$

Here  $\epsilon$  is random number between -1 and 1, it is cubed to make the peaks more drastic. The sinus curve is there to imitate the daily behaviour of the load and the period of 96 says that there is a measuring point every 15 minutes for 24 h. The constants were tweaked until the curve showed a behaviour that was comparable to real values taken from an operator. Since the function contains a random element it will look different every time, just as the actual load profile. An example of the profile can be seen in figure 4.12.

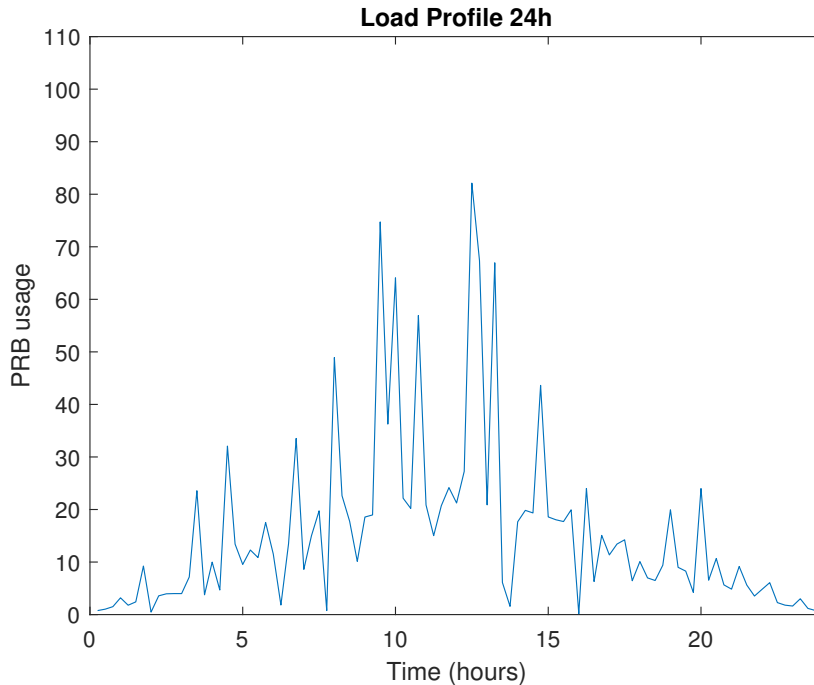


**Figure 4.12:** A random generated load profile based on equation 4.9 and inspired by data from a real suburban RBS. The graph shows a 24 h scenario starting from midnight.

The load profile in figure 4.12 is staying below 63 used PRBs at most times meaning that in this case the ECO-mode would be sufficient almost throughout the entire 24 h. But during a short period in the middle of the day the peaks are exceeding 63 PRBs. The PRB-utilization is reported every 15 minutes and it is therefore necessary to make a prediction for the coming 15 minutes. The first step is to look at the current value, if that is close or above 63 the ECO-mode has to be switched off. But it is also possible to make a prediction of what the next

value will be through a linear regression. In this example only two points are used, the slope is then calculated and can be used to estimate the next value. Another threshold is then set to this value and if either of these thresholds are reached the ECO-mode will switch off and the full bandwidth will be used.

Another challenge when switching is that it will introduce a small downtime of 60 ms, this means that should not be done too often. To prevent this a minimum off-time can be introduced. This means that when the ECO-mode has switched off it can not be turned on again until a certain period has passed regardless of the load. The described method can now be applied to the load in figure 4.12. This number of available PRBs are then plotted together with the load in figure 4.13. Since the backoff is either 0 or -2 dB the available PRBs can only take values of 100 or 63 which means that it is a hysteresis switch.

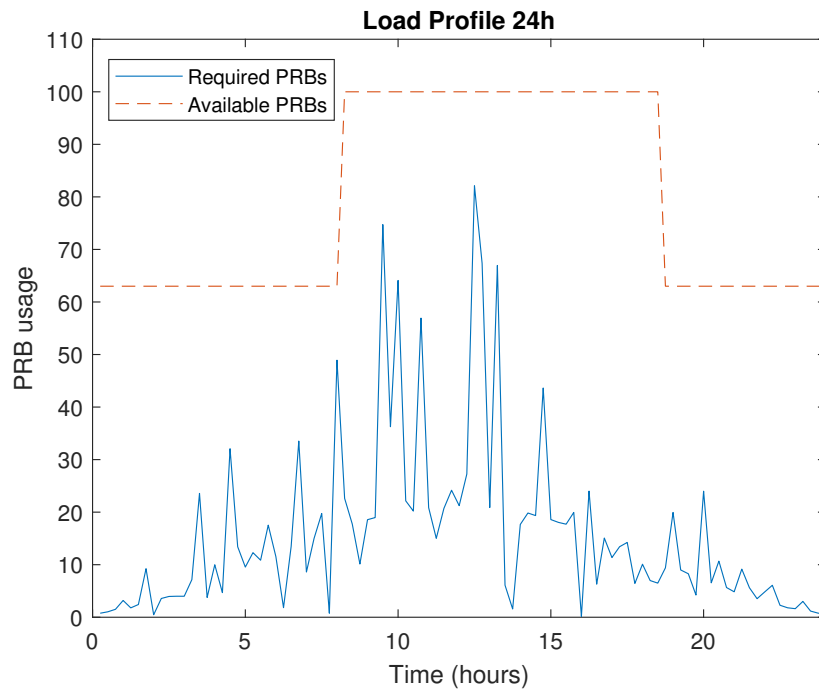


**Figure 4.13:** The upper graph shows the amount of available PRBs limited by the ECO-mode. The thresholds for switching off the ECO-mode are 50 for the last value, 60 for the predicted value and the ECO-mode has to be switched off for at least 5 hours.

In figure 4.13 one can see that the ECO-mode would be turned on during roughly half the 24 hour period. This is night time which is at the start and end of the period. The thresholds are set here as an illustrating example but it is possible to change them either to use the ECO-mode more or less. There is a

trade off here between power saving and the risk of having insufficient throughput for a period. If this simulation is run for a week with the same thresholds the result in figure 4.14 is obtained. In this case the ECO-mode is used 62% of the time and the time when there is a risk of insufficient throughput is 30 minutes over a week. During the third day of the simulation there are no large peaks meaning that there is no need for the ECO-mode to switch off.

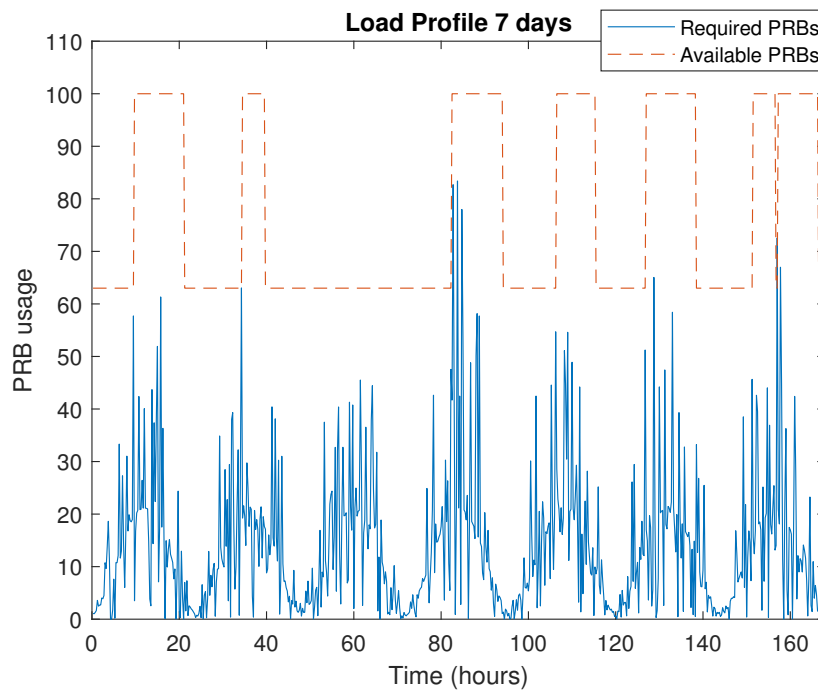


**Figure 4.14:** Simulated values for the load and ECO-mode over 7 days. The ECO-mode is used in 62% of the time and PRB-usage is higher than the available PRBs for 30 minutes.

## 4.7.2 Prototype

The effect of this simulation can be tried out in a script. It is written in the Ericsson tool interface called Moshell that is used to control the radio base station. This reads the amount of PRBs with constant intervals and is then taking a decision whether to have the ECO-mode on or off.

## PRB-utilization

The total amount of used PRBs are counted and reset every 15 minutes, called ROP-intervals. The value is updated every 6 seconds and the instant PRB-utilization can be derived from the difference between two measuring points. It was seen that 6 second intervals gave a large variation and the time was set to 30 seconds to get a good average. Since we are interested in the average PRB-utilization per TTI, that is 1 ms, the difference in a 30 second interval has to be divided by 30000.

## Prediction

After the first PRB-utilization is taken a loop will start. This loop calculates a new PRB-value and uses the two values to do a linear regression that will work as a prediction for the coming PRB-utilization. The last value and the prediction will now have a threshold level each and if either of these are reached the ECO-mode will be switched off. To switch on the ECO-mode again both the last value and the prediction has to be below the thresholds. This is used to be sure that it is safe to use fewer PRBs without the risk of not being able to supply throughput. Another feature that is added is a minimum time that the radio can be in the mode with no backoff, this is to make sure that it is not switching too often.

## Test method

The script with the adaptive backoff was tried out by applying a varying load through the Viavi. The different radios had different load profiles to visualize the effect of the ECO-mode, these load profiles are presented for each radio. The script has thresholds that will turn off the ECO-mode. The two thresholds are changed according to which radio that is used. In figure 4.6 it was seen that the backoff has a very small impact on the power consumption. Due to this result the adaptive ECO-mode would be hard to implement in a good way. The adaptive ECO-mode is therefore tested on radio B and C.

### 4.7.3 Radio B

It was seen in figure 4.9 that the ECO-mode saves power as long as it can sustain the throughput. This means that the thresholds should be placed in a level where they make sure that the radio can sustain the throughput. The threshold for the current PRB-utilization was set to 50 and the predicted to 57 in order to have some safety margin. Since the maximal throughput with ECO-mode is 86 Mbps a profile, seen in figure 4.15 with levels both below and above this value was chosen.

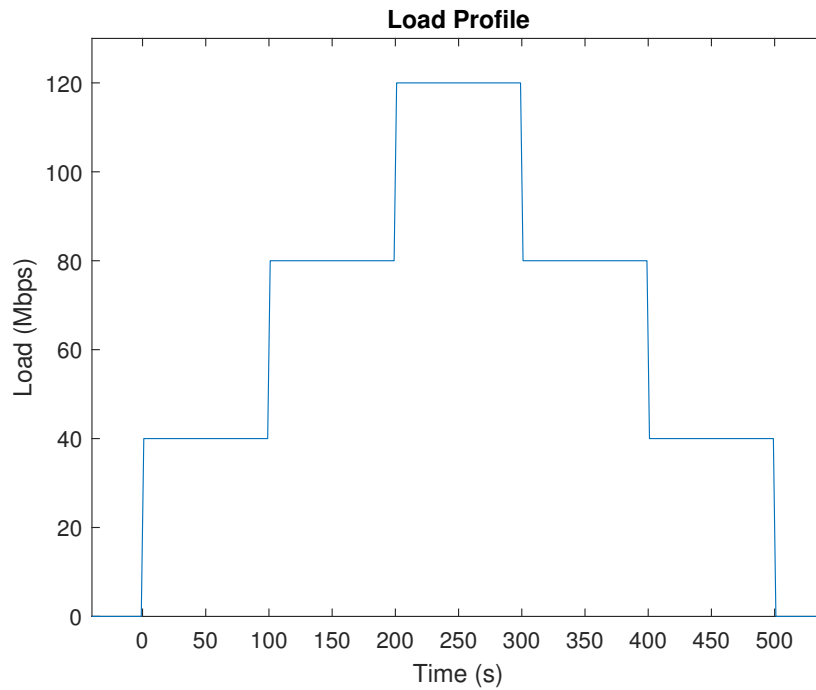


**Figure 4.15:** Load profile for the adaptive ECO-mode test. Three UEs are attached, each with 40 Mbps. They have different delays and duration to create a staircase formation.

This load profile was run both with and without the adaptive ECO-mode while measuring the power consumption. The result of this is seen in figure 4.16. When the load reaches 80 Mbps the ECO-mode is switched off since that is too close to the limit of what it can handle. The average power consumption was reduced with 3.4%.

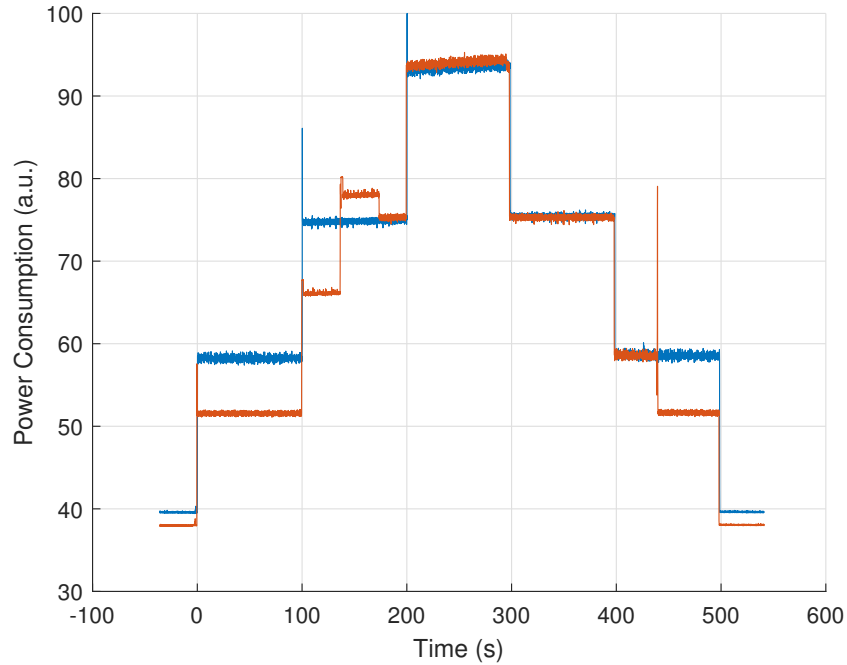


**Figure 4.16:** Comparison of the power consumption with and without the ECO-mode in a radio B. Both tests have Micro Sleep TX and LESS activated. When the adaptive ECO-mode is used the ECO-mode is turned on from the start. When reaching 80 Mbps it's turned off after 36 seconds and is remaining in that state for the highest load. When the load is coming back to 40 Mbps the ECO-mode is turned on after 39 seconds. The thresholds are set to 50 and 57 used PRBs for current and predicted value.

#### 4.7.4 Radio C

To introduce an adaptive ECO-mode with this radio the threshold levels would have to be lower. This will make the power saving less significant but since the PRB-utilization where the ECO-mode is ineffective is far from the ECO-mode maximal throughput the risk of having insufficient amount of PRBs is reduced. The thresholds are set to a PRB-utilization of 30 for both the current and the predicted value since this corresponds to roughly 35 Mbps when using 64 QAM, meaning that this is where the ECO-mode should be switched off. Another load profile seen in figure 4.17 is used to try out these new threshold levels. A comparison of the power consumption with and without the adaptive ECO-mode is shown in figure 4.18.

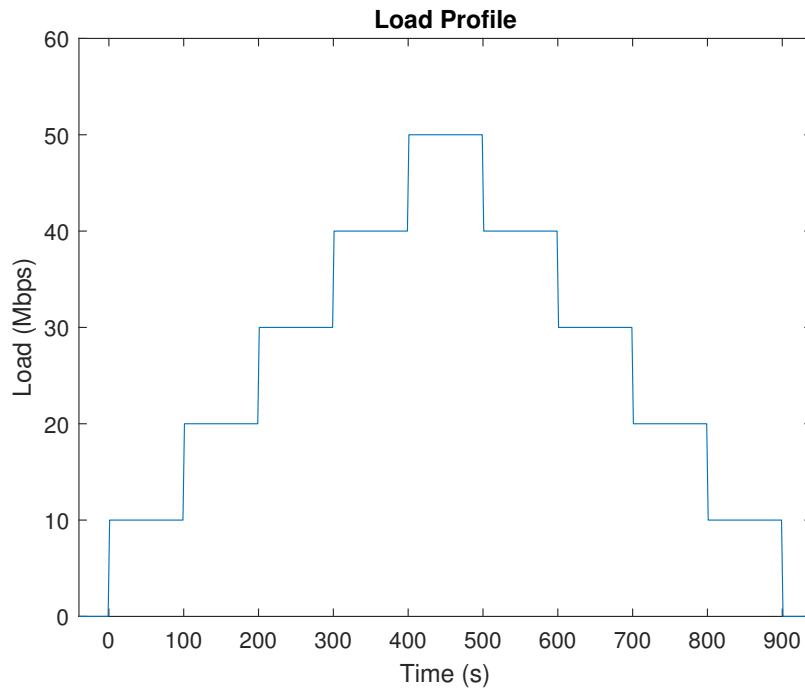


**Figure 4.17:** The load profile used to test the adaptive ECO-mode for radio C. The throughput is varied with the amount of UEs that are attached where each UE is using 1 Mbps.

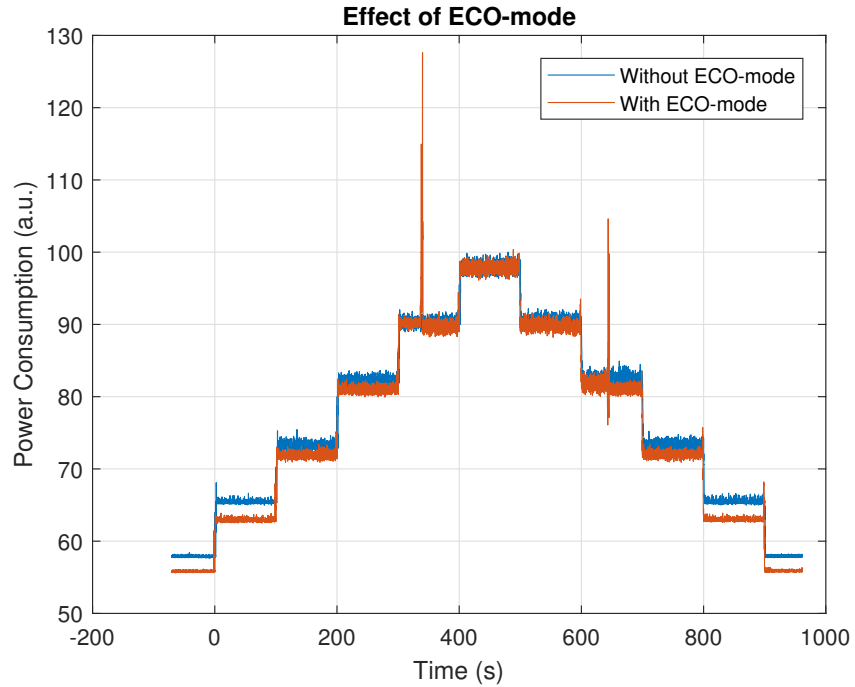


**Figure 4.18:** Comparison of power consumption with and without the adaptive ECO-mode. Both tests have Micro Sleep TX and LESS activated. The thresholds for switching on the ECO-mode are set to 30 for both current and predicted PRB-utilization.

#### 4.7.5 Results

The average power consumption for the RUs in this test case can be seen in table 4.3.

RU	Regular (a.u.)	Adaptive ECO-mode (a.u.)	Power save
Radio B	100	96.6	3.4%
Radio C	100	98.3	1.7%

**Table 4.3:** Average power consumption for the two RUs with and without the adaptive ECO-mode. The last column shows the power saving for each RU.



#### 4.7.6 Discussion

The power savings in table 4.3 are varying for the different radios where radio B shows the largest power save. One reason for this could be that Micro Sleep TX is less effective. This is because a radio with 4 branches has another CRS pattern meaning that more symbols are occupied in time domain which reduces the sleep time. It should also be stressed that most base stations are not running PSI-omni which means that there are several RUs at a particular site. The total power save is then obtained by multiplying the number by the amount of RUs at the site.

In this rather simple test cases the adaptive ECO-mode is able to follow the throughput well. This is helped a lot by slowly increasing the load so it has some time to recognise that it should switch. In the moment when the ECO-mode switches the power consumption has a short peak. The reason for this would have to be investigated further, but it's not large enough to mitigate the power save. If one looks at the top of the graphs one can notice a small slope meaning that the power consumption is increasing slightly even if the throughput stays the same. This is probably due to the slow temperature increase that happens at high load. A high temperature in the RU will increase the power consumption in the same way as for DU as explained earlier. It was also seen that decreasing the time interval for rebiasing of the PA resulted in a larger power save for radio C. It seems to work fine in the test case but it would need more verification in order to be implemented.



## Off grid solar design

---

### 5.1 Background

Alternative energy sources are used at RBSs that are beyond the reach of an electric grid, or where the electric supply is unreliable. Most commonly used energy source at such sites are the diesel generators. The regular maintenance and refuelling of diesel at these sites is difficult and gives rise to high operating expenses for the network operator. Large amounts of CO<sub>2</sub> emissions and local air pollution is also caused by these diesel generators.

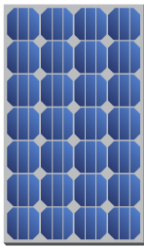
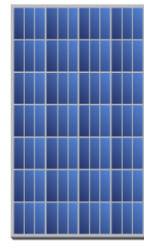
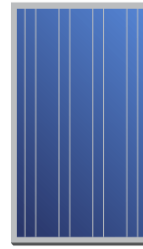
A lower power consumption at the RBS gives the opportunity to use renewable energy sources (like sun or wind) at the site. The size of a solar cell or a wind turbine is determined by the RBS load and by the availability of sun and wind at the site. This chapter focuses on the solar energy that is clean, requires almost no maintenance and is easy to install at the site. Therefore either an off-grid solar powered or a combination of solar and diesel would help the operators to bring down the expenses and emissions at the site.

### 5.2 Introduction

#### 5.2.1 Solar cells

Solar Cell or Photo Voltaic (PV) cell is a device made up of semiconductor materials such as silicon, gallium arsenide and cadmium telluride, etc. that converts sunlight directly into electricity. When the PV cell absorbs sunlight, free electrons and holes are created at the positive and negative junctions respectively. A bias is applied over the junction and the generated power can be calculated as the product of the bias and the generated current [15]. Silicon is the most used material and

these PV cells can be of different types such as mono-crystalline, poly-crystalline, thin-film or amorphous. The underlying material determines the cost and panel efficiency of the solar panel. The 3 types of solar cells are compared and consolidated in Table 5.1 [15, 16].

<b>Mono-crystalline</b>	<b>Poly-crystalline</b>	<b>Thin-film</b>
		
Manufactured from single Si crystal	Manufactured by fusing different crystals of Si	Manufactured by depositing one or more thin layers of Si material on the substrate
Most efficient with maximum panel efficiency of up to 21%	Less efficient than mono cells, has panel efficiencies up to 16%	Least efficient with maximum panel efficiency only up to 12%
Requires least area for a given power	Requires less area for a given power	Requires more area for a given power
Performs best at standard temperatures	Performs best at moderately high temperatures	Performs best at higher temperatures
Performance degrades in low sunlight conditions	Performance degrades in low sunlight conditions	Performance less affected by low sunlight conditions
Most expensive, takes more production time and costs	Lesser expensive than mono cells, takes lesser production time and costs	Least expensive, takes lesser production time and costs

**Table 5.1:** Comparison of different Solar Cell types

From the comparison in table 5.1, it can be seen that the main criteria for panel selection would be the panel efficiency, area required and the cost of the solar panels. The peak power (peak wattage) of a solar panel under standard test conditions is given by the equation

$$W_p = \eta_{PV} \cdot A_{PV} \cdot PSI \quad (5.1)$$

where  $\eta_{PV}$  is the panel efficiency,  $A_{PV}$  is the panel area and PSI is the Peak Solar Intensity, that is  $1 \text{ kW/m}^2$ . So for an RBS where sunlight and area are a limitation, it is better to use highly efficient mono-crystalline panels. Whereas at locations where there is ample sunlight and enough area, it will be cost effective to use poly-crystalline panels. Thin film panels would have been a good option in terms of their low sunlight requirement, cost and flexibility but its lower panel efficiency and larger area requirement makes it less popular among the solar panels. The mono and poly crystalline panels are manufactured and tested under standard conditions, hence they are more standardised and durable than the thin film panels.

## 5.2.2 Solar energy

The solar energy that falls on the solar panels is referred to as solar insolation or solar irradiance. The solar insolation is a measure of solar radiation energy received on a given surface area in a given time. It is expressed as average solar insolation or irradiance in kilowatt hours per square meter per day ( $\text{kWh/m}^2/\text{day}$ ). The average daily solar insolation is related to the Peak Sun Hours (PSH) at a given location. The PSH is the number of hours that the sun shines with PSI of  $1 \text{ kW/m}^2$ . This value is equivalent to the daily solar insolation at a particular location. That is for example, a location that receives an average solar insolation of  $5 \text{ kWh/m}^2$  per day is said to have received a peak solar radiation of  $1 \text{ kW/m}^2$  for 5 hours. Hence 5 hours is taken as the PSH for that location. This can also be illustrated in a graph as shown in figure 5.1 [17].

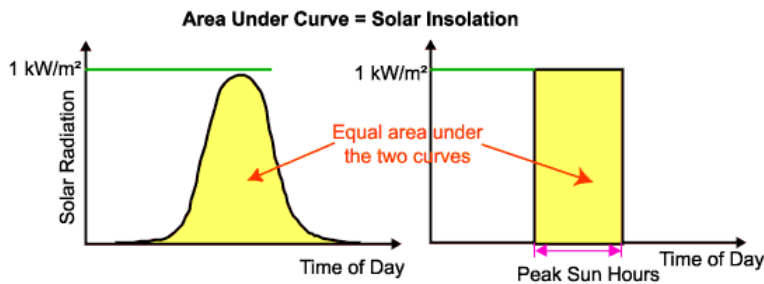


**Figure 5.1:** Solar insolation and Peak Sun Hours [17]

The power incident on a PV module depends on the PSI and the angle between the solar panel and the sun. As the angle between the sun and the surface of solar panel changes, it will change the power density on the PV module. The power density is said to be at its maximum when the absorbing surface is perpendicular to the sun. But the sun's radiation does not fall on a horizontal surface with the same intensity all throughout the day or year. Therefore a solar panel at an angle is a better option than a fixed horizontal panel. The amount of solar radi-

ation incident on such tilted panels is a component of the incident solar radiation perpendicular to the module surface. A number of other astronomical and geometrical factors also affect the amount of solar radiation, for example declination angle, zenith angle, latitude, longitude, season and other atmospheric conditions at a particular location [17]. In order to obtain an average optimal solar power throughout the year, the solar panel at a tilt angle equal to the latitude of the location is considered to be the best. The difference in average daily solar insolation incident on a horizontal and an optimally tilted surface at a location in southern Europe (Lisbon) for the whole year round can be seen in Figure 5.2.

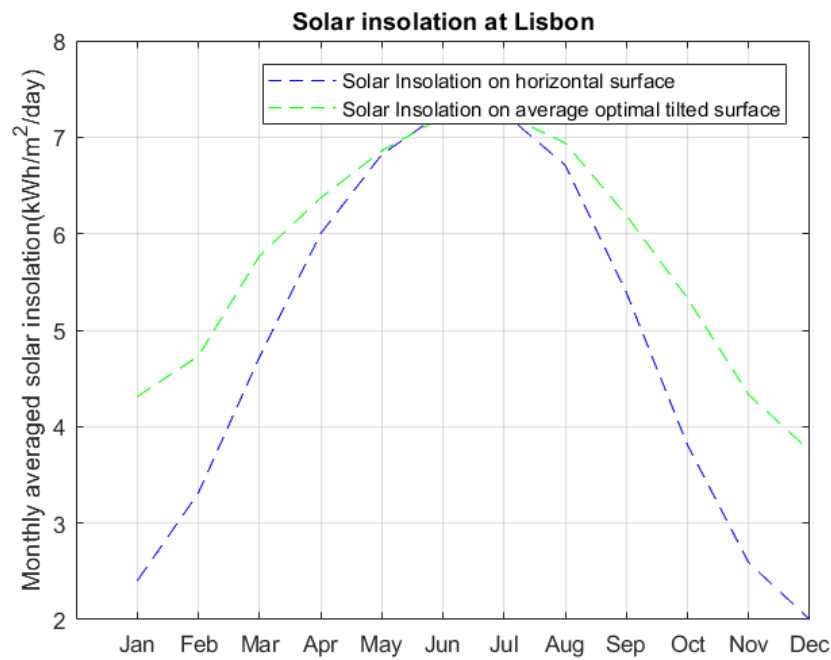


**Figure 5.2:** Solar insolation data on horizontal and an optimally tilted surface at a particular location

From the figure 5.2, it can be noticed that the average solar insolation values on a tilted surface are slightly higher than that on the horizontal surface. This is because the sunlight falls for more hours and with reasonable intensity on tilted panel than the horizontal panel. The solar insolation values also differs with the latitude and the time of the year. In countries closer to the poles, it has almost 24 hours of sunlight during summers and no sunlight at all in winters, this would mean that solar insolation is very high during summers and very low during winters. So in that case the solar panels would be more feasible during summers and not that much in winters. In countries closer to equator, the variation in sunlight during summers and winters is not so drastic hence the solar panels would be

suitable all throughout the year.

These solar data can be taken from the NASA's atmospheric science data centre or from similar meteorological databases [18, 19]. These values are needed to find the area and peak wattage of solar panels for a given load requirement. A world map showing the global horizontal irradiation pattern can be seen in Figure 5.3. This map shows the long term average of daily and yearly horizontal solar insolation at different parts of the world.

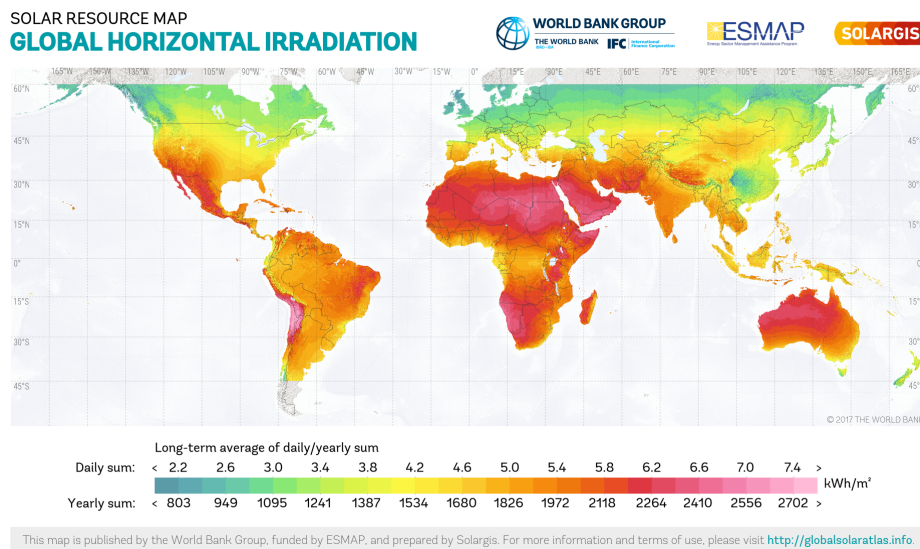


**Figure 5.3:** Global Horizontal Irradiation map

### 5.3 Solar PV system

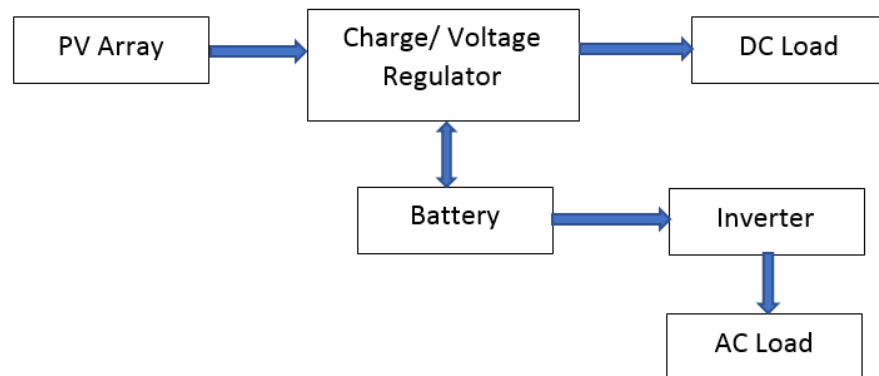
There are different ways to set up a solar PV system. It can be an off-grid/stand alone PV system, a grid connected/grid-tie PV system or an off-grid system with a combination of generators and solar/wind energy sources (hybrid system). The thesis will be discussing the basic design, feasibility and efficiency of an off-grid RBS. An off-grid solar PV system is set up with different modules that have to be designed and selected based on the energy requirement of the RBS. The major components of an off-grid solar PV system are listed here.

- PV module – consists of the solar panels that convert sunlight into DC electricity.
- Load – the combination of DC and AC electrical equipments that are con-

nected to the PV module and drawing energy from it. Here this will correspond to the RBS.

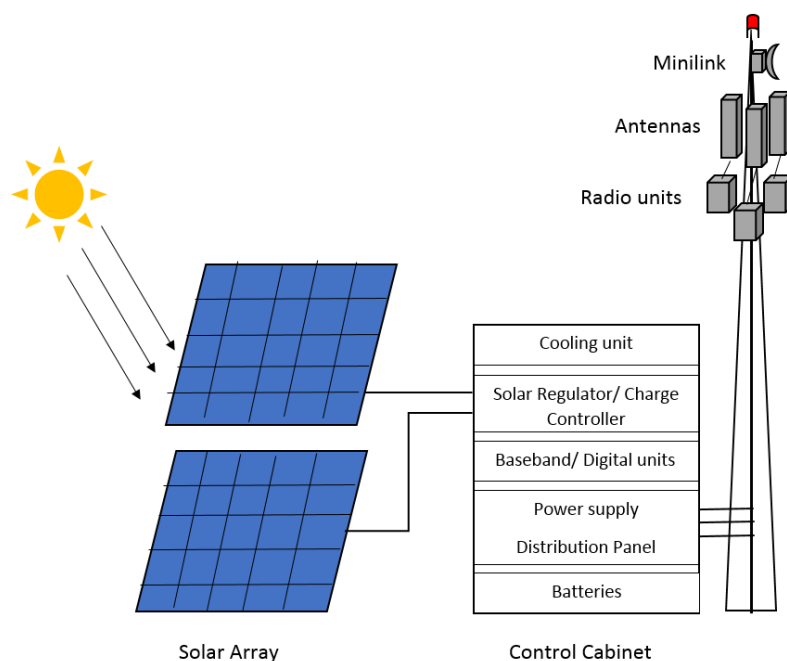
- Voltage/charge controller – regulates the voltage and current coming from the PV module and distributes it to the battery and the load. It sends the required energy to the load and the rest to the battery for storage. It also makes sure that the battery does not get overcharged and thereby prolongs the battery life.
- Battery – stores the extra energy from the PV module and supplies it to the load on demand, like during nights or on cloudy days when there is poor sunlight.
- Inverter – converts the DC output from the battery to an AC signal that is required for any AC load. Since an RBS itself is requiring DC current the inverter will only be used for additional equipment such as cooling or for generators.

Figure 5.4 shows the system block diagram of an off-grid PV system. It also shows the direction of flow of energy between the different modules. A typical set up of an off-grid solar powered RBS is shown in Figure 5.5



**Figure 5.4:** Off-grid PV system block diagram





**Figure 5.5:** Overall design of a solar powered RBS.

## 5.4 Off-grid PV system design

### 5.4.1 Solar Energy estimation

For the PV system design, depending on the location of the RBS site the average daily solar insolation and the PSH has to be found [18, 19]. The average solar insolation on an optimally tilted panel and the PSH derived from it is used for the calculations as those values are more precise and appropriate to the actual installation possible at an RBS. The maximum number of solar panels required for a site is calculated by considering the winter months, when the average solar insolation is the lowest. This is done in order to make sure that the solar panels would produce enough energy all the year round. The average solar insolation on an optimally tilted panel recorded at two different locations - one in northern Europe (Kista) and other in southern Europe (Lisbon) is shown in Figure 5.6. The variation here shows that Kista would require more number of efficient and higher peak power solar panels compared to Lisbon.

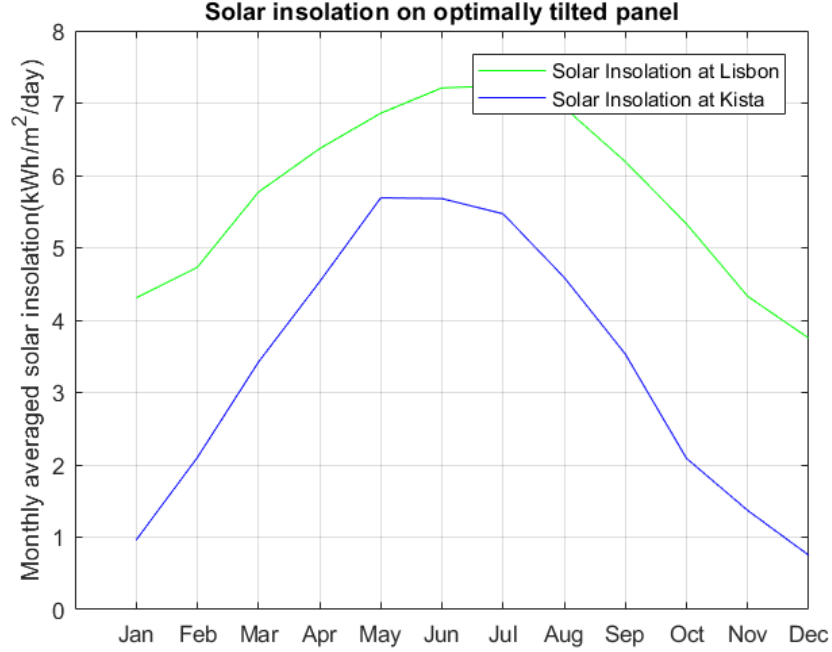


**Figure 5.6:** Average solar insolation on optimally tilted panel at two locations in Europe

#### 5.4.2 Load estimation

An off-grid solar RBS site is assumed to be set up as shown in Figure 5.5. It will consist of a control cabinet with the baseband/ digital unit (DU), cooling and power supply units in it and a mast on which usually 3 radio units (RU) and their antennas and the mini transmission link are connected. To design the solar PV system for such an RBS site, it is necessary to know the average daily load demand. The power consumption of the cooling unit, power supply unit, minilink and the baseband are mostly a constant for a particular RBS whereas the radio output power varies according to the traffic load as mentioned in Figure 2.1. The radio being the major contributor of RBS energy consumption, for the load estimation the variable load base station power model recommended in the EARTH (Energy Aware Radio and neTwork tecHnologies) project will be used [22] to calculate the radio unit power. This is a linear equation and is given by

$$Power = N_{TRX} \cdot (P_0 + (\Delta p \cdot P_{max} \cdot Avg_{traffic})) \quad (5.2)$$

where  $N_{TRX}$  is the number of transceivers. Here,  $N_{TRX}$  is  $2 \times 3 = 6$ , as the radios used in the thesis are configured with 2 transmitters and 3 sector receiver antennas.

$P_0$  is the power at idle state or no load when only CRS signals are transmitted and  $\delta p$  is the slope of power versus throughput. For the radios used in this thesis the slope was found to be in the range 0.75-1.25.  $P_{max}$  is the maximum output power configured in the radio, this is 40 W at maximum load and  $Avg_{traffic}$  is the average mobile traffic. In reality the mobile traffic varies a lot during the day, the traffic pattern in dense urban, suburban and rural areas are assumed as shown in Figure 5.7 [22]. The rural traffic pattern will be used for the design as the off grid sites are mostly in rural areas.

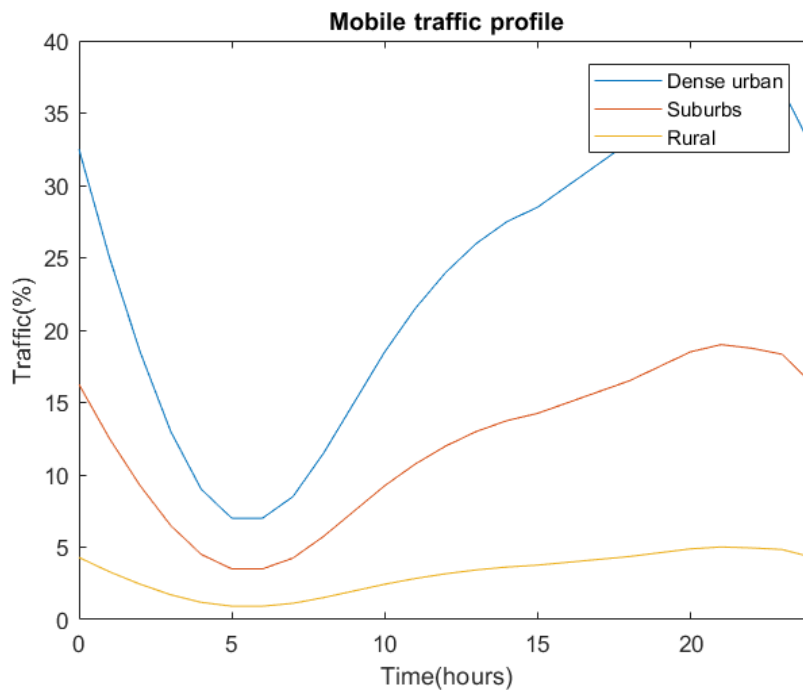


**Figure 5.7:** The mobile traffic pattern in urban, suburban and rural areas

Table 5.2 gives the radio unit power for two cases, one with regular radio and another with power save implemented radio. The values used here are taken from the radio B measurements mentioned in the previous chapter (Figure 4.9). To calculate the overall power demand of the site, the calculated radio unit power is added to the power consumed by rest of the modules. The power save by baseband cooling discussed in Chapter 2 is also considered here to see the overall power savings. The baseband cooling had reduced the power consumption by around 5 W at higher ambient temperatures. The Table 5.3 enumerates the power consumed by each of the different modules at the RBS and it showed that the power save features reduced the total power consumption at the site. The daily energy required in each case is also calculated by multiplying the total power by

24 hours.

Power mode	$N_{TRX}$	$P_0$	$\delta p$	$P_{max}$	$Avg_{traffic}$	RU Power
Regular (Reg)	6	130 W	1.2 W/Mbps	40 W	3.3 Mbps	1730 W
Power Save (PS)	6	105 W	0.9 W/Mbps	40 W	3.3 Mbps	1343 W

**Table 5.2:** Power consumption of the radio unit at a RBS

Modules	Reg	PS RU	PS RU + DU
RU (W)	1730	1343	1343
DU (W)	135	135	130
Cooling (W)	50	50	50
PSU (W)	100	100	100
Minilink (W)	25	25	25
Total RBS power (W)	2040	1653	1648
Daily Energy requirement (kWh)	48.96	39.67	39.55

**Table 5.3:** Total power consumption at a RBS

### 5.4.3 Battery size estimation

In order to choose an appropriate battery size for the RBS site, the daily Ampere hour (Ah) requirement has to be calculated first. This is found by dividing the daily energy requirement by the system voltage. Assuming daily energy requirement of 50 kWh for a regular site and 40 kWh for a power save site and system voltage of 48 V, it would require 1042 Ah and 833 Ah capacities respectively. This reduction in Ah capacity by power save will help to reduce the battery size. Next the number of days of back-up storage by the battery ( $Days_{auto}$ ) or the number of days of cloudy or unpleasant weather conditions has to be considered for the site. The decision on the number of days will also depend on the design of the PV array. The solar panel is either assumed to feed all the energy required by the load or it stores some part of the solar energy in batteries for those unpleasant days. Normally this value is taken as 2 or 3 days but for locations with highly unreliable weather conditions more days have to be considered. Depth of Discharge (DoD) is the maximum discharge that the battery will experience. It is also defined as the usable battery capacity that is limited by the load cut-off voltage of the battery. The DoD varies for different batteries, a lithium ion battery has a high DoD (90%) compared to the common lead acid batteries (50-80%). Finally the efficiency of the battery ( $\eta_B$ ) has to be considered, this is the efficiency of the battery when it is charging and discharging. A round trip efficiency of 85% is considered for the calculations [23, 24, 25]. Now the actual battery capacity for the regular and power save site can be found by using the equation given by




$$Ah_{actual} = \frac{Ah \cdot Days_{auto}}{DoD \cdot \eta_B} \quad (5.3)$$

Considering 2 autonomous days, DoD of 90% and battery efficiency of 85%, the actual battery capacity for the regular and power save RBS was calculated and it was found to be 2724 Ah and 2178 Ah respectively. The number of series and parallel connected batteries will depend upon the selected system voltage and the rated battery capacity respectively. Table 5.4 gives the different rated battery capacities and the number of batteries required in each case for the given specifications.

Rated battery capacity(Ah)	Number of batteries	
	Regular	Power Save
50	54	44
100	27	22
150	18	14
250	11	9
500	5	4

**Table 5.4:** Number of Battery modules

There are different types of solar batteries available in the market, the most common ones are compared and consolidated in table 5.5 [30, 31].

Lead Acid	Lithium ion	Salt water
		
Has lesser DoD 50-80%	Higher DoD (80-90%)	Higher DoD
Expels hydrogen gas due to the chemicals in it	Lesser emissions	Lesser emissions and more eco friendly as it uses salt water
Requires more recharging	Faster charging and discharging	-
Flooded batteries require more maintenance compared to sealed batteries	Not much maintenance required	Not much maintenance required
Lifespan of 5-7 years	Lifespan of more than 10 years	Lifespan of up to 8 years
Least expensive	Most expensive	More expensive than Lead acid batteries

**Table 5.5:** Comparison of different Solar Batteries

#### 5.4.4 PV array estimation

The peak power rating of the solar panels and the area required for a solar powered RBS site depends mainly on the energy requirement of the site and the location of the site. The location of the site is related to its PSH that will help to find the power rating. The least PSH recorded at the location is used to find the maximum peak power rating of the solar panel. The losses due to dirt, snow or shade on the panels (5%), temperature losses (3%), dc and ac cable losses (4%), radiation losses (5%), device losses(3%) etc. have to be considered for the design. Here a minimum value of all these losses ( $\sigma_{loss}$ ) are taken for the calculation, but for the actual site design these losses have to be taken into account depending on the location of site, type of solar panels and devices etc. The system efficiency comprising of charge controller ( $\eta_{CC}$ ) and battery ( $\eta_B$ ) efficiency are also considered in order to find the actual energy that needs to be provided by the solar panel. The PV peak power is calculated using equation given by

$$Wp_{PV} = \frac{E_{req}}{(1 - \sigma_{loss}) \cdot \eta_{CC} \cdot \eta_B \cdot PSH} \quad (5.4)$$

A 25% higher margin is assumed in order to have enough energy to charge the battery and supply the load even during the worst sunny days. This assumption will make sure that the batteries have enough charge to run the RBS at night. Total losses of 20%, battery efficiency of 85% and charge controller efficiency of 95% are considered and PSH corresponding to solar insolation on tilted panel is used for the calculations. The number of parallel connected solar panels will depend upon the selected rated PV system power and here a standard 250 Wp solar panel is selected for the calculation. The panel area required for the site is then calculated using the equation 5.1 where the panel efficiency is taken as 16% for the 250 Wp solar panel. Table 5.6 lists the solar insolation (PSH) values found for different months in Kista and the maximum peak power (Wp) required and area required for each month.

Months	PSH (hr)	Wp required (kW)		Area required (m <sup>2</sup> )	
		Regular	Power save	Regular	Power save
Jan	0.96	98.8	79.8	158.0	127.7
Feb	2.1	45.1	36.5	72.2	58.4
Mar	3.42	27.7	22.4	44.4	35.8
Apr	4.53	20.9	16.9	33.5	27.1
May	5.69	16.7	13.5	26.7	21.5
Jun	5.68	16.7	13.5	26.7	21.6
Jul	5.47	17.3	14.0	27.7	22.4
Aug	4.59	20.7	16.7	33.1	26.7
Sep	3.53	26.9	21.7	43.0	34.7
Oct	2.09	45.4	36.7	72.6	58.7
Nov	1.37	69.2	55.9	110.7	89.5
Dec	0.75	126.4	102.2	202.3	163.5

**Table 5.6:** Maximum peak power and area of solar panel required for the different months of the year in Kista

Similarly, Table 5.7 lists the solar insolation (PSH) values found for different months in Lisbon and the maximum peak wattage (Wp) and area required for each month.

Months	PSH (hr)	Wp required (kW)		Area required (m <sup>2</sup> )	
		Regular	Power save	Regular	Power save
Jan	4.31	22.0	17.8	35.2	28.4
Feb	4.73	20.0	16.2	32.1	25.9
Mar	5.77	16.4	13.3	26.3	21.2
Apr	6.37	14.9	12.0	23.8	19.2
May	6.86	13.8	11.2	22.1	17.9
Jun	7.21	13.2	10.6	21.0	17.0
Jul	7.24	13.1	10.6	21.0	16.9
Aug	6.94	13.7	11.0	21.9	17.7
Sep	6.19	15.3	12.4	24.5	19.8
Oct	5.33	17.8	14.4	28.5	23.0
Nov	4.33	21.9	17.7	35.0	28.3
Dec	3.75	25.3	20.4	40.5	32.7

**Table 5.7:** Maximum peak power and area of solar panel required for the different months of the year in Lisbon

Maximum Wp required at Kista is 126.4 kW for a PSH of 0.75 whereas in Lisbon, the maximum Wp is only 25.3 kW, this is due to the higher PSH and better sun conditions even during winters at Lisbon. It can be noticed that the power save features reduces the maximum Wp and it reduces to 102.2 kW and 20.4 kW for Kista and Lisbon sites respectively. The maximum number of 250 Wp solar panels that would be needed to provide power save, maximum Wp at these sites would be approximately 400 and 80 respectively. From the very high values of peak wattage during the winter months (Nov, Dec, Jan) at Kista, it is clear that the solar panels are not a suitable solution for sites closer to poles and hence an alternate solution has to be thought of for such places.

#### 5.4.5 Solar charge/ voltage controller estimation

The solar charge/voltage controller is used to regulate the current and voltage from the PV array and send the required current and voltage to the batteries and the load. This module helps in preventing the battery from overcharging and prolongs the battery life. There are mainly two types of charge controllers- Pulse Width Modulated (PWM) and Maximum Power Point Tracking (MPPT) charge controllers. The PWM controller is like a switch that is used to control the voltage and current from solar array to give the required voltage and current output to the battery and the load. Whereas the MPPT controller is more sophisticated and expensive than PWM. Here the controller will adjust the voltage from the PV array so as to obtain the maximum power from it. This power is then used to supply the varying voltage requirements of the battery and load [28]. To find



the rating of the charge controller, the maximum rated current of the controller has to be calculated using the solar panel short circuit current. A safety margin of 25% is added here to account for any sudden variations [23, 24, 25]. If the 250 Wp solar panel is selected, the short circuit current for it is 8.15 A, the Kista site would require a maximum rated current of  $1.25 \cdot 8.15 \cdot 400 = 4075$  A and Lisbon site would require a maximum current of  $1.25 \cdot 8.15 \cdot 66 = 815$  A. These high values of current are obtained for the maximum, worst case Wp conditions. This current can be reduced and distributed between the battery and load by using a number of charge controllers.

#### 5.4.6 Inverter size estimation

Until now the only load that has been discussed is requiring DC power. If there are any AC power requirements the design would require an inverter to do the DC to AC conversion. Inverters have to be used in cases where we connect the load to a diesel generator or to run an air conditioner in the cabinet. The inverter power rating in those cases is calculated by assuming a 25% higher AC power requirement [23, 24, 25]. Assume a site with 2 kW diesel generator, it would require an inverter of rating  $1.25 \cdot 2 \text{ kW} = 2.5 \text{ kVA}$ .

#### 5.4.7 Cable size estimation

Copper cables have to be used to connect the different modules in the RBS. The cable area is calculated using the basic Ohm's law. Here the acceptable losses have to be considered as there will be a drop in voltage and hence a drop in power when current flows over a distance through the cable. The voltage drop index (VDI) is a reference number based on resistance of the cable that is used to calculate an appropriate American wire gauge (AWG) specification of the cable. The area of the conductor is determined by the current carrying capability or ampacity of the conductor [34, 35]. VDI is given by

$$VDI = \frac{I \cdot L}{\%V_d \cdot sys_{volt}} \quad (5.5)$$

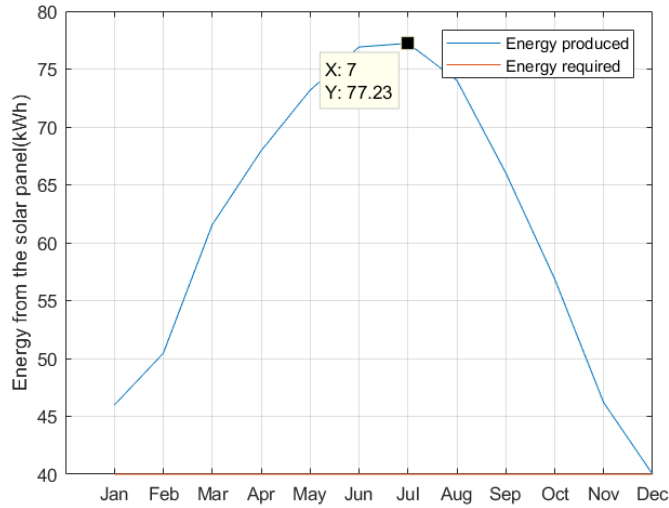
where  $I$  is the maximum current through the cable (A),  $L$  is the one way wiring distance of the cable (in feet),  $V_d$  is the acceptable voltage drop say 2% expressed as 2 and  $sys_{volt}$  is the system voltage that is 48 V here. Let us assume that a site requires a 5 m cable to connect the solar panels to the charge controllers. It has to carry a maximum current of say 100 A with an acceptable voltage drop of 2%. VDI is obtained as 17, taking the nearest VDI value equal to 20, a copper wire of 4 AWG with an area of more than  $22.2 \text{ mm}^2$  would be required.

#### 5.4.8 Design summary

A basic design of each of the modules in an off-grid solar site is presented and in all the module designs it clearly showed that the power save features helped to reduce the size of the modules and this would definitely reduce the costs involved at the site. By following certain guidelines the PV system installations could be made more effective and less costly [24]. This includes

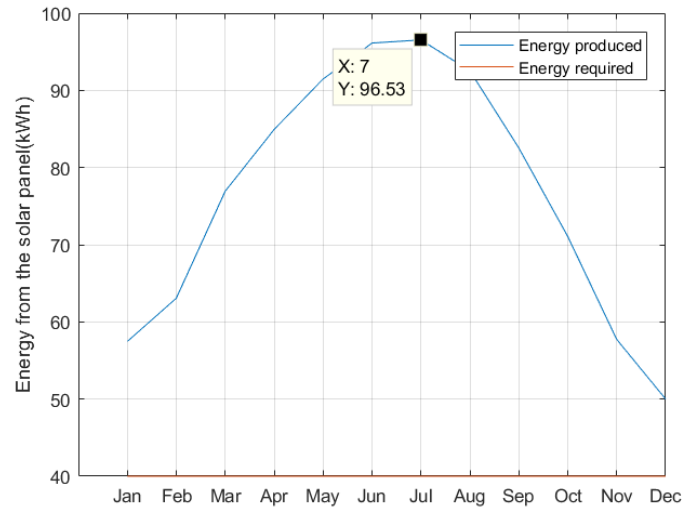
- Proper selection of the site without any shade and having enough area to tap required energy for the site. Less shade means lesser losses and appropriate area of very efficient solar panels would give energy as per requirement.
- The orientation and mounting of PV modules are very critical for generating the required energy, hence the solar panels have to be installed at correct tilt angle and in correct direction of sun in order to maximise the PV output and the solar insolation gain.
- Load determines the size of the PV system, so the load has to be kept within a limited range by proper planning of the site and by using power save features on the load. This would avoid having bulky modules and thereby higher costs for the site.
- Battery storage and battery selection is very important for the site as the battery storage determines the self sustainability of the site. The number of days of back up will vary for different sites and the battery selected for storage will affect the actual battery size required for a site.
- PV modules have to be selected according to the site's maximum peak wattage requirement. The worst case design values were presented in the previous section. Depending on the solar conditions at the site, the efficiency and type of panel has to be selected as the solar panel's peak wattage is directly proportional to the panel efficiency and solar intensity.
- The charge controllers for the solar site has to be selected to operate efficiently while meeting the needs of both the battery and load.
- The cables at the site should be selected such that it minimises the voltage drop between the modules.

The power save energy requirement and the maximum  $W_p$  required for each month at Lisbon, will give an energy demand graph as shown in figure 5.8.



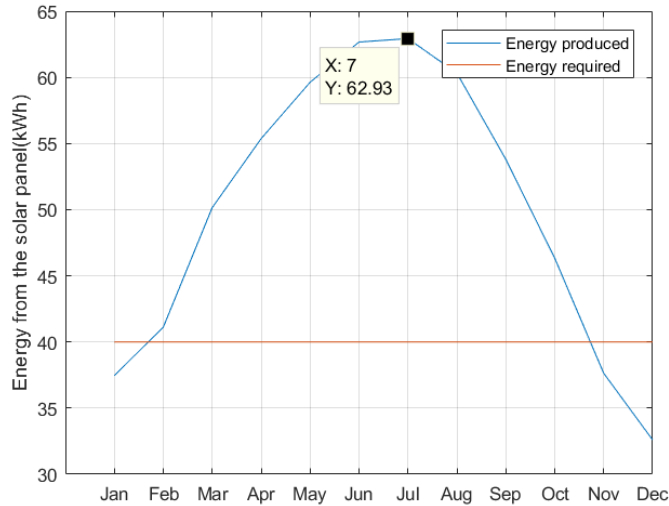
**Figure 5.8:** Energy demand by load

Figure 5.8 shows the constant energy required by the load and the energy provided by the solar panels during different months of the year. It can be seen that the solar panels provides just enough energy to the load during the least sunny month of December. To design a self sustainable PV system such that it charges the battery along with feeding the constant load, a 25% extra has to be added to the daily energy requirement. This safety margin can be seen clearly for the month of December in the Figure 5.9.



**Figure 5.9:** Energy demand by load and battery with safety margin

But in both the above cases, it can be noticed that during summer months the solar panels generate surplus energy after feeding the load and charging the battery. This surplus energy will get wasted if not put into use. This excess energy can be made use for some solar powered water pump or street lighting in the rural locality of the site. Another way to overcome this situation is to take annual average PSH instead of least PSH for PV array estimation. On assuming annual average PSH, the excess energy during summer months is reduced as shown in figure 5.10, but the solar panels are unable to feed the load requirement for few months.



**Figure 5.10:** Energy demand by load and battery with annual average PSH

It is at this situation that an alternative solution - a combined system which includes a diesel generator along with the PV system might be helpful. So for few months the diesel generator would supply the RBS whereas for rest of the months the solar panels would supply the necessary power. Instead of powering the RBS fully on diesel or solar, this combined option might seem to be a better alternative as it would reduce number of solar panels, the days of maintenance and refuelling of diesel for the operators.

## 5.5 Cost analysis

The high capital and operating expenses and the environmental concerns due to the off grid diesel power solution has been a major concern to the network operators. The off grid solar solution could be a better solution in terms of environment but it depends on the solar conditions whether it is feasible in terms of cost. Another alternate solution of having a combination of both diesel and solar could be the most effective solution as both the costs and the emissions can be reduced effectively with such a set up. A cost analysis of RBS powered by fully solar, fully diesel and a combination of both is performed to identify the best option among the three power options for an off-grid RBS.

In the previous sections, the design of the different modules for two RBS sites in Europe have been discussed. These designs have been done with both regular

and power save radio and baseband units. The regular site requires energy of approximately 50 kWh/day whereas the power save site requires approximately 40 kWh/day as mentioned in Table 5.3. To calculate the total annual cost in each case the costs are divided into two categories - investment costs and yearly costs. The investment costs includes total cost of each of the modules and the cost of setting them up at the site. The yearly costs include the maintenance and fuel costs. The annuity of the investment costs are calculated using equation 5.6 for a given lifetime and discount rate. The annuity of the investment is taken due to the fact that the cost of the modules will change over a period of time at a certain discount rate. Once the annual investment costs are found the yearly costs are added to it to obtain the total annual cost of the site.

$$A = \frac{r \cdot CV}{1 - (1 + r)^{-n}} \quad (5.6)$$

where,  $r$  is the depreciation rate (10%),  $n$  is the lifespan (20 years) and  $CV$  is the current value.

For the cost analysis few assumptions on the costs are taken and they are as follows

- The cost of solar panel is assumed to be \$1/W<sub>p</sub> [29, 30].
- The cost of solar battery is assumed to be \$209/kWh.
- The cost of charge controller is assumed to be \$75/kW.
- The cost of solar inverter is assumed to be \$0.55/kVA.
- The cost of solar installation is assumed to be 10% of the solar panel cost [26].
- The cost of diesel generator is assumed to be \$1000/kW [27].
- The cost of installation of diesel generator is assumed to be 25% of the diesel generator cost.
- The cost of solar panel maintenance per year is assumed to be 2% of the solar panel cost [26].
- The cost of maintenance in diesel generator per year is assumed to be 3% of the diesel generator cost [27, 36].
- It is assumed that 1 liter of diesel is used to generate 10 kWh of energy, this along with 30% efficiency of the generator gives 30 kWh of energy per litre [36].
- The fuel cost is assumed to be \$2/litre and this includes the fuel refilling costs too.

### 5.5.1 Solar powered system

A fully solar powered RBS site will have a set up as shown in figure 5.11. The design of an RBS site in Lisbon is considered for the cost analysis first. Here 25% higher margin with system efficiency of 80.75%, losses of 20% and least PSH of 3.75 is used for the maximum solar peak wattage calculation. A maximum peak wattage of 25 kW<sub>p</sub> and 20 kW<sub>p</sub> is obtained for the regular and power save sites respectively for the worst sunny months in Lisbon. The cost of the PV modules is calculated using the cost assumption \$1/W<sub>p</sub> and it is obtained as \$25000 for regular and \$20000 for power save site. A lithium ion battery with capacity to sustain 2 days, with DoD 90% and efficiency 85% is considered for the battery costs. A battery capacity of 131 kWh and 105 kWh is required for the regular and power save site respectively. By multiplying these values with \$209/ kWh, we obtain \$27379 and \$21945 for the regular and power save. The charge controller should be able to control a maximum power of  $1.25 \cdot 8.15 \cdot 48 \cdot 100 \approx 50$  kW in a regular site whereas  $1.25 \cdot 8.15 \cdot 48 \cdot 80 \approx 39$  kW in a power save site. These values are multiplied with \$75/ kW to get the costs as \$3750 and \$2925 respectively. In the installation costs, the cost of setting up each of the modules is considered and in the maintenance cost, the cost of cleaning the panels, cost of replacement of batteries etc. are taken into consideration. Once the cost of each of the modules is calculated, the installation cost is found which is 10% of PV modules cost. The annuity of this total cost is calculated and added with the maintenance costs which is 2% of PV modules cost to find the total annual cost. Table 5.8 lists the cost of all the modules, installation costs and annuity calculated for the investment in the top portion and the maintenance costs are added to this in the lower portion.

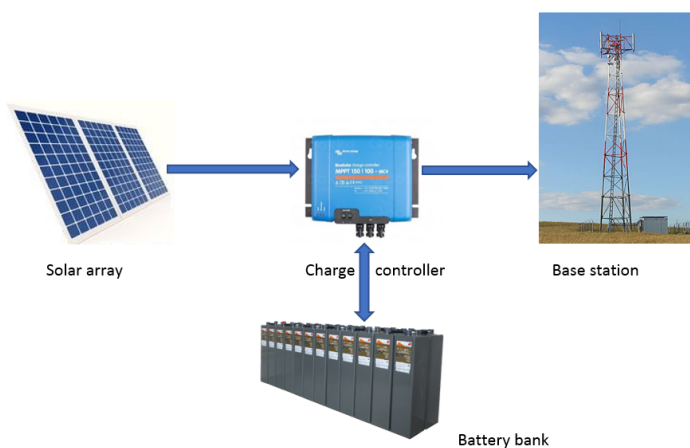


**Figure 5.11:** Fully solar powered site set up

Module	Regular	Power save
PV modules	25000	20000
Battery	27379	21945
Charge controller	3750	2925
Installation	2500	2000
Total investment	58629	46870
Annuity	6886	5505
Maintenance	500	400
Total annual cost	7386	5905

**Table 5.8:** Comparison of costs in a solar powered base station with and without power save features, all values are given in American dollars.

The table clearly shows that the power save features reduces the total annual costs for the operators. Here except for the batteries, rest of the costs are found to be less and for a site with more average sun hours throughout the year these costs would become even lower. Since there are less environmental concerns related to the solar site and it can be made use for pumps and street lighting in the rural locality, this option is much better than the diesel which gives out a lot of emissions.

### 5.5.2 Diesel powered system

A fully diesel powered RBS site will have a set up as shown in figure 5.12. For the diesel generator design one has to choose an appropriate size of the generator. Larger diesel generators can usually run for more hours and here a generator that will supply the RBS for 20 years is selected to make it comparable with the solar cells. The total energy consumption of the RBS for 20 years is found by multiplying the daily average energy by the number of days, this comes to 365 MWh and 292 MWh for the regular and power save sites respectively. From [27] it is seen that a generator of size 15 to 50 kW is able to run for 10000 hours, which is enough to supply the RBS for 20 years. A 36.5 kW and 29.2 kW generator is required by the regular and power save sites respectively and hence the generator costs would be \$36500 and \$29200. The generators are usually not run for a whole day, they are run only once or twice daily, hence the diesel powered site would require a battery. A small lithium ion battery with a capacity to sustain half a day, with DoD 90% and efficiency 85% is considered and a battery capacity of 24 kWh and 19 kWh is obtained for the regular and power save site respectively. The battery costs is then found to be \$5016 and \$3971. The generator produces AC current while the base station requires DC, hence an inverter is required to do this conversion. A 36.5 kW generator would require  $1.25 \cdot 36.5 \text{ kW} \approx 46 \text{ kW}$  inverter and 29.2 kW generator would require  $1.25 \cdot 29.2 \text{ kW} \approx 37 \text{ kW}$  inverter. The inverter costs for both the



sites would then be \$25300 and \$20350 respectively. The total investment cost includes the cost of the diesel generator and other modules and the installation costs. The installation cost includes the cost of setting up the site and it is taken as 25% of the generator cost that is \$9125 and \$7300 for the two sites. The total investment cost is now calculated and the annuity is found to be \$8920 and \$7144. The yearly maintenance and fuel costs of the diesel are then added to this annuity to find the total annual cost. The maintenance cost of diesel includes the cost of changing filters, oil, fuel etc. and this is taken as 3% of the generator cost that is \$1095 and \$876 respectively. In order to find the yearly costs of fuel and refilling, one has to know the amount of diesel used in an year. A diesel generator has an efficiency of 30% and one liter of diesel is assumed to withhold 10 kWh of energy therefore the amount of diesel required per year can be calculated using the equation given by

$$Fuel = \frac{E_{req} \cdot 365}{0.3 \cdot 10} \quad (5.7)$$

Using the equation 5.7, a regular site would require 6083 litres of diesel a year whereas the power save site would require 4867 litres of diesel a year. The fuel costs would then be \$12166 and \$9734 for the sites and this is then added to the investment and maintenance costs to find the total annual costs of the site. Table 5.9 lists the cost of the modules, installation costs and annuity calculated for the investment in the top portion and the maintenance costs and fuel costs are added to this in the lower portion.



**Figure 5.12:** Fully diesel powered site set up

Module	Regular	Power save
Diesel generator	36500	29200
Battery	5016	3971
Inverter	25300	20350
Installation	9125	7300
Total investment	75941	60821
Annuity	8920	7144
Maintenance	1095	876
Fuel	12166	9734
Total annual cost	22181	17754

**Table 5.9:** Comparison of costs in a diesel powered base station with and without power save features, all values are given in American dollars.

From Table 5.9 it can be seen that the diesel site needs much bigger modules and they incur higher investment costs compared to the solar site. It can also be noticed that the fuel costs take the major portion of the total annual costs. The high costs involved and the environmental concerns due to emissions from the generator makes this a bad option to the operators and hence another alternate solution which is less costly and more environment friendly has to be found.

### 5.5.3 Solar-Diesel hybrid system

A combination of solar and diesel could probably be a better alternate solution for the RBS sites in terms of cost and environment. Here the costs and the environmental effect will be analysed for the combined system. The solar and diesel hybrid system will have set up as shown in Figure 5.13. From the tables 5.8 and 5.9 it is found that a solar powered site is cheaper than an off-grid diesel site in Lisbon. When calculating the annual costs for a site in Kista in the similar manner, the total annual costs for the solar solution was found to be \$24187 and \$19554 for the regular and power save site respectively. The annual price of the diesel solution will not change significantly which means that the solar cells are not economically viable for this site. A cost analysis with the combination of solar and diesel solution is carried out to check if that is a better and cost effective solution for Kista.



**Figure 5.13:** Solar diesel hybrid site set up

In a solar-diesel hybrid system design few months of the year are powered by solar cells and rest of the year will be powered by diesel. For the cost calculations for a combined system in Kista, the power save site is considered and a combination of the costs in fully solar and diesel powered systems are used. The energy generated by the solar cells is subtracted from the total energy required by the site to obtain the energy that has to come from the diesel generator. This is calculated for various amounts of solar cells and the result is obtained as shown in Figure 5.14. It is seen that the cost for the solar design is increasing when more solar cells are added and the cost of the diesel generator is reduced with increasing number of solar cells and the least total annual cost was found with 75 solar modules, giving an annual price of \$7466. This value is smaller than the costs obtained for fully solar and fully diesel solutions in Kista. This cost analysis was repeated on the Lisbon site to see the costs for a combined solution. The Lisbon site had the least total annual cost of \$3029 with 60 solar modules as shown in Figure 5.15. So assuming Lisbon and Kista to be having two extreme sun conditions, this analysis will help us to find a break point for the cost effective combination of solar and diesel. Since Kista and Lisbon has got a minimum in between 60-75 solar modules, the use of 70 solar modules and rest by a smaller diesel generator should give the least cost for sites having least PSH values between 0.75 and 3.75. Fewer number of solar modules, smaller capacity batteries, inverter and generator would bring down the total module costs. The fuel costs would also be reduced drastically as the generators would be used only during few months and for lesser time. This will also reduce the emissions from the generator.

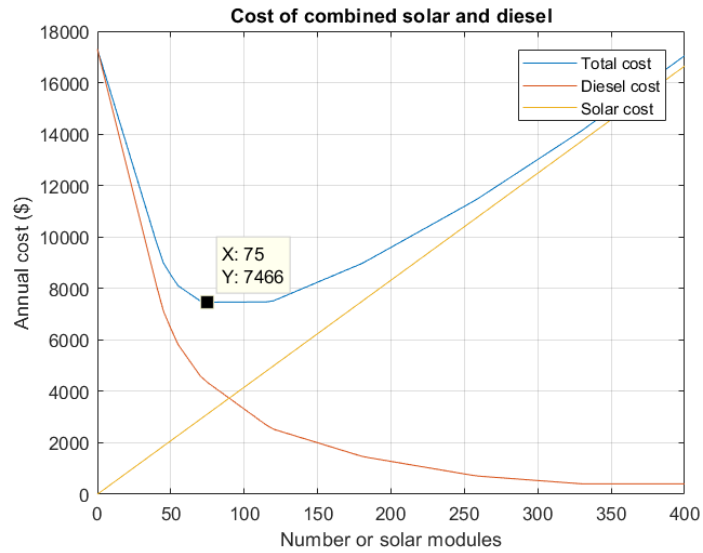


**Figure 5.14:** Cost trend for a combined solar cell and diesel powered RBS in Kista. The RBS is assumed to use all power save features and has an energy consumption of 40 kWh per day

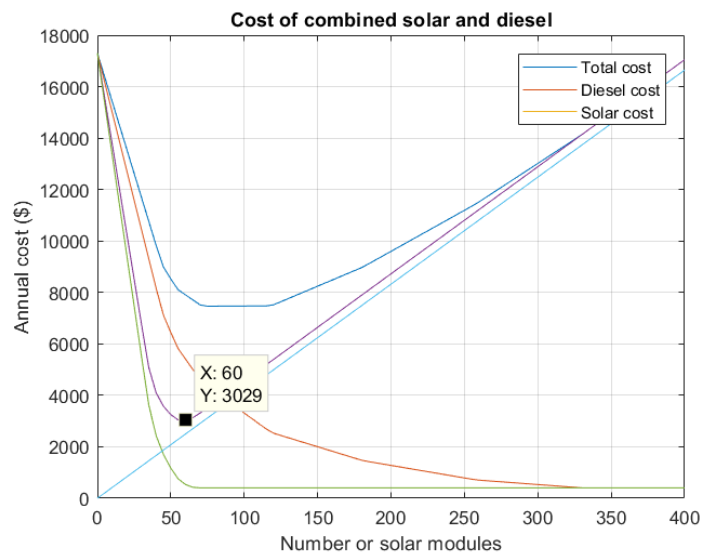


**Figure 5.15:** Cost trend for a combined solar cell and diesel powered RBS in Lisbon. The RBS is assumed to use all power save features and has an energy consumption of 40 kWh per day

To analyse the exact difference in emissions, the  $CO_2$  emissions given out in both cases can be calculated. One litre of diesel gives out 2.6 kg of  $CO_2$  or GHG emissions [32], which means that a fully diesel powered RBS that needs 4867 litres of fuel annually will give out 12654 kg of  $CO_2$  emissions. When an optimal combined solar - diesel system with power save features is used, the energy from diesel generator can be found out as the difference between the energy requirement of the site and energy supplied by the solar modules. This value is found to be 22.5 kWh. A diesel generator that provides 22.5 kWh of energy per day would require 2737 litres of fuel per year using equation 5.7. Hence the emissions reduces to 7116 kg which is almost half of the earlier case. Hence an RBS site with power save features incorporated and powered partly by solar and rest by diesel will be energy efficient, cost effective and less harmful to the environment.

#### 5.5.4 Summary on cost analysis

It was seen in the cost analysis that for a base station in a sunny environment an off-grid solar design is feasible and cheaper than the diesel generator when comparing the annual costs. For a location with less sun hours during parts of the year a combined solution was found to be the cheapest. When using both the power save features and the optimal power source solution the annual costs can be reduced from \$17754 to \$3029 in a Mediterranean environment and down to \$7466 in locations closer to the poles. It should, however, be noted that the values assumed in these calculations can vary depending on the brand of different devices or the country that the RBS is located in. But this analysis would give a good overview over the main costs in a solar or diesel powered base station. Table 5.10 gives the overall comparison of the three power options analysed in this section and it is clear that the combined solar and diesel option has been better on all aspects related to the RBS site.

	<b>Solar</b>	<b>Diesel</b>	<b>Combination</b>
<b>Module sizes</b>	Large (poles), small (equator)	Large	Reduced
<b>Capital costs</b>	High (poles), low (equator)	High	Reduced
<b>Operating costs</b>	Low	High	Reduced
<b>Fuel costs</b>	No fuel	High	Reduced
<b>Emissions</b>	No emissions	High	Reduced

**Table 5.10:** Comparison of the different power options analysed in this section.

A lot of countries have regulations and taxes that favours renewable energy sources and penalises carbon dioxide emissions. These have not been taken into account but it would most likely make annual savings even larger. One could also look into the future where the efficiency of solar cells will increase due to techniques like multi-junctions, where various semiconductor materials are used.

This will reduce the cost of the solar design even further. The diesel on the other hand being a finite energy source, it will become more inaccessible and more expensive in the near future. But even when disregarding the economical benefits of using solar cells, companies could also gain goodwill making them look better in the public opinion and create good marketing points.

## Discussion

---

In this ending chapter the results and conclusions of the thesis will be discussed. Some other ideas that was discussed during the thesis are presented and there are also some suggested further steps.

### 6.1 Conclusions

The two energy efficiency methods here are both saving significant amounts of power. This can reduce the operators energy bills but it could also reduce GHG emissions in sites where fossil fuels are used. The baseband cooling optimization has showed to be most effective in sites where the ambient temperature is high. But since it will make sure that the power consumption in the baseband is at its lowest at all times it is suitable for any climate and to be run continuously independent of other factors. The ECO-mode on the other hand will require the ability to switch on and off depending on the load. This makes it a more challenging to use but the power save in each RU can be rather large. It has also been seen that the ECO-mode is more efficient in RUs where Micro Sleep TX gives a low power save. This is expected since the ECO-mode is saving power by reducing the frequency spectrum while LESS and Micro Sleep TX wants to pack as much data as possible in the frequency domain to free up TTIs. But even when Micro Sleep TX is as most effective the ECO-mode can save power at low load, which is the most common scenario for most base stations. The basic considerations required for the off grid solar PV site design has been analysed. The energy efficient radio and baseband units proved to be beneficial for a solar powered RBS as less power means lesser number of solar panels and area for installation, fewer number of bulky components and lower costs altogether. The cost analysis with the different power options showed that a fully diesel powered site incurred more costs than fully solar or a combined power system. It also showed that by combining solar and diesel power options the annual cost of the site could be reduced by 38% in locations like Kista where the sun conditions vary a lot through the year. The

combined power option also reduced the fuel costs and GHG emissions by 56%.

## 6.2 Other ideas

During the introducing weeks of the thesis several other ideas regarding power efficiency were discussed. Some of these are listed in this section. It is also explained why we decided to not proceed with them.

### 6.2.1 RBS location

In a lot of areas the base stations are located close together to increase throughput. This is not always optimised for energy efficiency. The idea here was to look at the size and location of the base stations and see if this can be optimised. If the cell size is larger the Inter Site Distance (ISD) can be larger meaning that fewer base stations have to be used. So there is a trade off between size and number that could be modelled depending on the surrounding environment and the load profile of the site. Some minor simulations were done in Matlab but we did not proceed any further with this idea. The main reason was that a lot of the limiting factors when it comes to cell planning has to do with other parts than the technique itself. It has to do with who owns the land or the building that the base station is desired to be put on. We didn't want to spend the thesis looking at legal issues and decided to put this idea away.

### 6.2.2 Smoothing of load

As explained earlier the load varies a lot over the day. It is almost always peaking during the day and it's low during the night. Since the operator wants to satisfy its users even at peak hours the sites have to be designed for the peak hour load. This means that most base stations have an average load that is far lower than its full capacity. If the load during the peak hours could be reduced a smaller base station would be required which would save energy for the system. To reduce the peaks we thought of an idea where all low priority data could be scheduled to send during low load hours. This could include things like scheduled downloads of software upgrades or data from IoT-devices that only has to report once or twice a day. But with some machine learning and good prediction of the users more data can be used. An example of this could be a user that reads a digital newspaper every morning, the news could then load continuously over the night instead of resulting in a sharp peak in morning. Another case would be user who is watching tv series through a streaming service, it is likely that the he or she will watch the next episode and it could therefore be downloaded during low load hours. The main problem with this is that it could interfere with the user experience, it would



also be hard to do from the base station side and would rather be something that the operator could look at.

### 6.2.3 Modulation

When studying modulation it is often said that a higher modulation requires more energy. This assumes that the higher modulation is adding points further out in the scheme seen in figure 1.4 and will therefore require a larger amplitude. The idea was then to use the lowest possible modulation for the desired throughput to save energy. We then learned that in this case the modulation works in the opposite way. The dots in a higher modulation scheme are added inside, closer to the origo point of the scheme. This means that the average power per symbol stays roughly the same but since more bits can be transmitted in a higher modulation the power is used more efficient. The data can then be packed harder and LESS can be used more, the result is that power is actually saved at higher modulation.

### 6.2.4 Beam forming

Beam forming is, as explained in chapter 1, used to direct the signals towards a specific user. Our idea here was to instead use the beam forming in idle mode to shape the cell. In the current situation the cells are circular. But if the CRS signals could be directed in a desired direction the cell could have a longer reach there and the cell would appear to be oval instead of circular. This would increase the possibilities when doing cell planning and perhaps smaller or fewer base station could be used in some cases. Since this beam forming is not as precise as when it is directed towards a particular UE it doesn't require as much computing power. Due to similar reasons as for the RBS locations we did not proceed any further with this idea.

### 6.2.5 Increase the delay time of LESS

In its current state LESS has a maximum delay time of 20 ms, meaning that data cannot be delayed more than this no matter how many PRBs that are filled. But for some low priority data such as web pages or emails it would be acceptable to have a much larger delay time. We thought that increasing the delay could increase the impact of LESS and therefore save energy. But after doing some more reading we found that it would probably have a really small impact since the scheduler is almost never waiting 20 ms. This is because one of the other thresholds in the LESS configuration is usually met before.

## 6.3 Further steps

Even if the power saving features discussed in this thesis have shown significant power savings in the lab at Ericsson some more investigation would have to be made before using it in practice.

### 6.3.1 Baseband cooling

One would have to take a closer look at the MTBF for the fan when it has a higher average speed. It would also be valuable to study the impact on the components on the board when they are having a lower average temperature. To further optimize the adaptive fan speed one could tweak the step size or even make the step size itself change to make it catch quick temperature variations with a good accuracy. This could maybe be done with some machine learning since the temperature variations look different at different sites.

### 6.3.2 ECO-mode

For this power save feature there are some more optimization to be done regarding the adaptive mode. As a start one could tweak the thresholds to save as much power as possible without affecting the throughput. As seen this is different for different RUs but it could also be different regarding the location of the site since the load profile may vary. How drastic the peaks are is going to affect how conservative one has to be when choosing thresholds. Another problem with this mode is that it has a downtime when switching. If one could manage to reduce this or even to make the transition entirely seamless there is a possibility of using several backoff steps. In that sense the PA could do an envelope tracking and the power consumption would scale much better with the load.

### 6.3.3 Solar PV design

A small solar site could be set up in the lab and the actual design and measurements could be carried out. The actual variations in design can be checked with the help of such a prototype. In this thesis a fixed efficiency has been used but there is a lot of research going on to improve the efficiency and reduce the costs of solar cells. Analysis considering a higher efficiency and thus higher rated power might give another result that could favour the solution with pure solar power.

---

## References

---

- [1] A. Krumbein. (2016). *Understanding the Basics of MIMO Communication Technology*.
- [2] Ericsson. (2016). *The Future of Mobile Subscriptions, Ericsson Mobility Report* <https://www.ericsson.com/en/mobility-report/future-of-mobile-subscriptions>
- [3] LTE Resource Grid. [http://niviuk.free.fr/lte\\_resource\\_grid.html](http://niviuk.free.fr/lte_resource_grid.html)
- [4] LTE Signaling: Troubleshooting and Optimization. <http://ltesignaling.blogspot.com/2012/02/link-adaptation-in-lte.html>
- [5] L. Frenzel. (2013). *Understanding Error Vector Magnitude*. <http://www.electronicdesign.com/engineering-essentials/understanding-error-vector-magnitude>
- [6] I. Shayea, M. Ismail, R. Nordin. (2013). *Downlink Spectral Efficiency Evaluation with Carrier Aggregation in LTE-Advanced System Employing Adaptive Modulation and Coding Schemes*.
- [7] T. Haynes. (1998). *A Primer on Digital Beamforming*.
- [8] M Dardaillon et al. (2013). *Cognitive Radio Programming: Existing Solutions and Open Issues*
- [9] a) S. Lambert, W. Van Heddeghem, W. Vereecken, B. Lannoo, D. Colle, and M. Pickavet. (2012). *Worldwide electricity consumption of communication networks*
- [10] K. Tweed *Why Cellular Towers in Developing Nations Are Making the Move to Solar Power*. Scientific American. (2013).
- [11] J. Lorinez, T. Garma and G. Petrovic. (2012). *Measurements and Modelling of Base Station Power Consumption under Real Traffic Loads*.
- [12] B. Berglund, J. Johansson and T. Lejon. (2006). *High efficiency power amplifiers*.

- [13] M.J. Scott, L. Fu, X. Zhang, J. Li, C. Yao, M Sievers & J. Wang. (2013). *Merits of gallium nitride based power conversion. Semiconductor Science and Technology.* 28. 074013. 10.1088/0268-1242/28/7/074013.
- [14] Ericsson Baseband. [https://www.ericsson.com/ourportfolio/networks-products/baseband?nav=fgb\\_101\\_0561\%7Cfgb\\_101\\_0516](https://www.ericsson.com/ourportfolio/networks-products/baseband?nav=fgb_101_0561\%7Cfgb_101_0516). Taken: 2018-05-25.
- [15] [http://www.leonics.com/support/article2\\_13j/articles2\\_13j\\_en.php](http://www.leonics.com/support/article2_13j/articles2_13j_en.php)
- [16] <http://energyinformative.org/best-solar-panel-monocrystalline-polycrystalline-tl>
- [17] <https://www.pveducation.org/pvcdrom/average-solar-radiation>
- [18] <https://power.larc.nasa.gov>
- [19] <https://solargis.com/maps-and-gis-data/download/world>
- [20] *Power Consumption Guideline for RBS 6000*
- [21] Master Thesis - Kousthubh Sharma (2017). *Comparison of energy efficiency between macro and micro cells using energy saving schemes*
- [22] Gunther Auer (DOCOMO), Oliver Blume (ALUD), Vito Giannini (IMEC), Istvan Godor (ETH), Muhammad Ali Imran (UNIS), Ylva Jading (EAB), Efstathios Katranaras (UNIS), Magnus Olsson (EAB), Dario Sabella (TI), Per Skillermark (EAB), Wieslawa Wajda (ALUD), INFISO-ICT-247733 EARTH Deliverable D2.3 *Energy efficiency analysis of the reference systems, areas of improvements and target breakdown*
- [23] Ishaq M., Ibrahim U.H., Abubakar, H.(2013). *Design Of An Off Grid Photovoltaic System: A Case Study Of Government Technical College, Wudil, Kano State* INTERNATIONAL JOURNAL OF SCIENTIFIC and TECHNOLOGY RESEARCH VOLUME 2, ISSUE 12
- [24] Parimita Mohanty, K. Rahul Sharma, Mukesh Gujar, Mohan Kolhe and Aimie Nazmin Azmi. (2013). *PV System Design for Off-Grid Applications*
- [25] Marwan M. Mahmoud\*, Imad H. Ibrik. (2006). *Techno-economic feasibility of energy supply of remote villages in Palestine by PV-systems, diesel generators and electric grid* Elsevier Renewable and Sustainable Energy Reviews 10
- [26] Abd El-Shafy A. Nafeh(2009). *Design and economic analysis of a stand alone PV system to electrify a remote area household in Egypt* The Open Renewable Energy Journal, 2
- [27] J. Kurtz, G. Saur, S. Sprik, and C. Ainscough National Renewable Energy Laboratory Backup Power Cost of Ownership Analysis and Incumbent Technology Comparison
- [28] <https://www.victronenergy.com/blog/2014/07/21/which-solar-charge-controller-pwm-or-mppt/>
- [29] <https://www.civicsolar.com/support>

- 
- [30] <https://www.wholesalesolar.com/solar-information>
  - [31] <https://www.energysage.com/solar/solar-energy-storage/what-are-the-best-batteries-for-solar-panels/>
  - [32] [https://energyeducation.ca/encyclopedia/Diesel\\_generator](https://energyeducation.ca/encyclopedia/Diesel_generator)
  - [33] <https://www.eia.gov/petroleum/gasdiesel/>
  - [34] <http://www.solar-wind.co.uk/cable-sizing-DC-cables.html>
  - [35] <https://www.altestore.com/howto/wire-sizing-tool-for-12-24-and-48-volt-dc-systems-a106/>
  - [36] <https://www.facilitiesnet.com/powercommunication/article/Onsite-Options-Facility-Management-Power-Communication-Feature--1679>
  - [37] <https://www.globalpwr.com/power-calculator/>
  - [38] <https://www.homerenergy.com/products/pro/docs/>